Report prepared for:

SANTOS LTD
91 King William St
Adelaide
SA 5000

PETROLOGY REPORT

CALLISTER-1

OTWAY BASIN
(VIC/P 51)

Report prepared by:

Dr S E PHILLIPS
PGPC
1c Short Crescent
Beaumont SA 5066

May 2005

Mobile: 0414 712 728 Fax/phone: (61) 08 8379 8281 Email:pgpc@bigpond.com.au

CONTENTS

PAGE

Front cover:
Thin section photomicrograph, Callister-1, MSCT 20, depth 3471.0m. Plane light. Horizontal field of view 1.30mm.

1. SUMMARY

Santos Ltd submitted 15 MSCTs to Phillips-Gerrard Petrology Consultants from Callister-1 in the Otway Basin. Samples were selected from the Late Cretaceous Waarre Formation for detailed petrological description, point counting and grain size analysis. The study was design to ascertain the lithology, mineralogy, sediment provenance, depositional environments, diagenetic alteration and factors controlling reservoir quality.

Sandstones from Callister-1 are very fine to medium grained, poor to well sorted litharenites and feldspathic litharenites. Muddy siltstones are also apparent and interbedded with the sandstones. Lithologically the sandstones are very similar to those previously described from Unit A in the Waarre Formation at the Casino Field.

Sediment at Callister-1 was derived dominantly from a metamorphic terrane with lesser igneous influence. Sedimentary lithics are less abundant and had a more continuous source. There are more lithics and feldspars than at Casino, possibly as a result of proximity to the source but the types of lithics and feldspars are almost identical. At the base of the sequence in Callister-1 an increase in metamorphic lithics corresponds to an increase in K-feldspars, whilst the percentage of both igneous lithics and plagioclase decline. Above approximately 3600 to 3550m all the feldspars and igneous + metamorphic lithics show a more constant decline in abundance. It is thought that this break in sedimentation may have been associated with tectonic activity in the metamorphic terrane. Very similar trends were apparent in the Casino Field and may reflect regional trends in the tectonostratigraphy across the Mussel Platform.

A marine to marginal marine depositional environment of either a lower delta plain influenced by distributary channels and/or a delta front is envisaged for sediments from Callister-1. This interpretation is based on a combination of the petrology data and wireline logs. Burrows and possible faecal pellets may indicate a location above fair weather wave base. Initial deposition probably occurred close to a river mouth as indicated by the presence of chlorite rims. Trace amounts of immature and rarely oxidised glaucony and pyrite framboids reflect the marine setting and possible reworking of sediments. Shallower sediments contain relatively high percentages of Fe rich micrite associated with organic matter and detrital clays which might suggest a more terrestrial influence.

Trends in early diagenetic alteration (glaucony, framboidal pyrite, chlorite, Fe rich carbonate and oxidation) were related to the depositional environments. After burial the sediment was subject to compaction, dissolution and precipitation of kaolin, illite, quartz and clear carbonate spar. Some of these later events were probably influenced by the break in sedimentation. Dissolution of feldspars might be related to flushing by meteoric waters after uplift. Corrosion of Fe rich carbonate could have occurred in association with the initial pulse of CO_2 associated with localised Pleistocene to Recent volcanism and subsequent later precipitation of clear carbonate spar. There was no evidence of carbonate dissolution nor development of chlorite rims in the Casino Field. Feldspar overgrowths noted at Casino have not developed at Callister-1.

Poor reservoir quality at Callister-1 is the result of primary intergranular pores being occluded by compaction, and to a lesser degree cementation. Porosity is dominated by secondary dissolution pores (grain size, honeycomb and intragranular) which are poorly interconnected. Remnants of primary intergranular pores are preserved where there are chlorite rims at depth, or quartz overgrowths in shallower samples and all these samples have minor permeability. Micropores associated with kaolin and chlorite do contribute to total porosity but this may not be effective porosity.

2. INTRODUCTION

Santos Ltd submitted 15 mechanical sidewall cores to PGPC from the well Callister-1 in the Otway Basin (VIC/P51). Samples were selected from the Late Cretaceous Waarre Formation for detailed petrological description. The study was design to ascertain the lithology, mineralogy, sediment provenance, depositional environments, diagenetic alteration and factors controlling reservoir quality.

The services listed below (Table 1) were provided by PGPC. To aid the petrology interpretation the client supplied a wireline log of the selected interval, formation tops, preliminary porosity and permeability data and a map showing the well location.

TABLE 1 SUMMARY OF SAMPLES & SERVICES

MSCT	Depth (m)	Unit	TS description	Grain size analysis	Point count
3	3858.0	Waarre A	*	*	*
4	3849.5	Waarre A	*	*	*
5	3809.5	Waarre A	*	*	*
6	3802.0	Waarre A	*	*	*
7	3791.0	Waarre A	*	*	*
9	3700.0	Waarre A	*	*	*
10	3695.5	Waarre A	*	*	*
11	3620.0	Waarre A	*	*	*
12	3614.0	Waarre A	*	*	*
15	3535.0	Waarre A	*	*	*
16	3526.5	Waarre A	*	*	*
17	3482.6	Waarre A	*	*	*
18	3481.0	Waarre A	*	*	*
20	3471.0	Waarre A	*	*	*
21	3464.0	Waarre B	*	*	*

3. METHODS

Thin section

Mechanical sidewall cores were impregnated with araldite prior to thin section preparation by Petrographic Technical Services Pty Ltd. Blue dye was used in the araldite to facilitate description of porosity and permeability. Thin sections were prepared using standard techniques to produce a thickness of 30 microns (Adams *et al*, 1984). Thin sections were systematically scanned to determine lithology, composition, porosity and textural relationships. Siliciclastics have been classified according to guidelines by Folk (1974). Grain morphology (both sphericity and roundness) was estimated by comparison with charts in Pettijohn *et al* (1987), grain fabric (packing and texture) from the diagram in Tucker (2001) and sorting from diagrams by Harrell (1984). All percentages of composition given in Table 2 are counts of 500 points following the method of Stanton & Wilson (1994). The basic data for grain size analyses was collected by measuring the long axis of 100 representative grains in thin section. The graphic mean, mode and inclusive graphic standard deviation (Folk, 1974) were then calculated.

4. PETROLOGY

TABLE 2 POINT COUNT DATA FOR CALLISTER-1

MSCT	3	4	5	6	7	9	10	11
Depth (m)	3858	3849.5	3809.5	3802	3791	3700	3695.5	3620
Framework grains								
Quartz - mono	31.4	19.4	26.0	25.2	19.0	20.6	27.0	26.4
- poly	4.4	3.8	3.8	2.2	3.4	5.0	7.0	4.0
Feldspar - Kspar	1.8	8.8	7.0	5.8	6.4	6.8	6.4	3.6
- plagioclase	3.0	5.0	3.6	1.6	2.4	2.8	1.8	1.2
Lithics - sedimentary	0.4	4.0	3.0	5.0	5.6	4.2	6.0	2.0
- metamorphic	5.0	11.6	11.4	13.8	18.6	16.2	18.6	11.0
- igneous	0.6	13.8	13.2	8.8	12.2	11.2	9.2	2.6
- unknown	2.2	1.6	0.8	1.4	1.8	5.2	1.2	0.0
Mica - muscovite	4.4	1.4	0.4	1.0	1.4	0.6	1.6	3.6
- biotite	3.0	0.8	0.4	1.4	0.8	0.6	1.0	2.2
Accessory - zircon	0.6	0.2	0.2	0.2	0.2	0.2	0.2	0.2
- tourmaline	0.2	0.2	0.0	0.0	0.0	0.2	0.2	0.0
- rutile	0.6	0.4	0.0	0.0	0.0	0.0	0.0	0.2
- opaques	0.6	0.6	0.0	0.0	0.0	0.2	0.0	0.0
- garnet	0.0	0.0	0.2	0.2	0.0	0.0	0.0	0.0
- ?monazite	0.0	0.0	0.0	0.0	0.0	0.0	0.2	0.2
Matrix								
Clay	23.8	0.4	0.0	0.0	0.8	0.0	0.6	22.8
Organic matter	4.2	0.4	0.0	2.6	0.6	0.4	1.2	5.8
Authigenic minerals								
Glaucony	1.0	0.6	0.0	0.8	0.2	1.8	0.2	1.0
Chlorite - replace	3.8	4.8	4.8	2.4	3.4	5.6	1.4	8.2
- fill pores	0.0	8.2	8.4	6.0	9.6	4.8	1.2	0.0
Fe Carbonate - replace	5.2	0.0	0.0	0.0	0.0	0.0	0.8	2.8
- fill pores	0.0	0.0	0.0	0.0	0.0	0.0	0.0	0.0
Clear Carbonate - replace	2.6	1.8	2.4	2.6	2.0	1.4	3.0	1.0
- fill pores	0.0	0.4	1.0	1.2	2.4	0.0	2.2	0.0
Quartz	0.0	0.0	0.2	0.4	0.4	0.0	1.2	0.0
Illite - replace	0.0	0.0	0.0	0.2	0.0	0.0	0.0	0.0
Kaolin - replace	0.0	0.0	0.0	3.2	0.2	2.2	1.2	0.0
- fill pores	0.0	0.0	0.0	3.8	0.2	2.4	0.4	0.0
Oxide	1.0	1.0	0.0	0.0	0.0	2.8	0.0	0.0
Pyrite - replace	0.0	0.0	0.0	0.0	0.0	0.2	0.0	0.0
- fill pores	0.0	0.0	0.0	0.0	0.0	0.2	0.0	0.0
Porosity								
Intergranular	0.0	5.4	7.8	4.6	3.8	0.8	1.0	0.0
Dissolution	0.0	5.0	5.0	4.8	4.0	3.0	5.0	1.2
Shrinkage	0.2	0.0	0.0	0.0	0.0	0.2	0.0	0.0
Micropores	0.0	0.4	0.4	0.8	0.6	0.4	0.2	0.0
TOTAL	100.0	100.0	100.0	100.0	100.0	100.0	100.0	100.0

TABLE 2 POINT COUNT DATA FOR CALLISTER-1 continued

MSCT	12	15	16	17	18	20	21
Depth (m)	3614	3535	3526.5	3482.6	3481	3471	3464
Framework grains							
Quartz - mono	24.4	25.4	32.2	29.0	33.6	29.4	34.4
- poly	6.0	2.8	3.2	3.4	4.2	4.8	3.8
Feldspar - Kspar	8.0	3.4	4.4	3.6	5.4	4.6	6.4
- plagioclase	1.2	1.2	1.2	1.0	0.8	1.0	0.8
Lithics - sedimentary	4.0	1.4	3.0	1.4	2.6	4.0	3.6
- metamorphic	19.4	7.2	9.4	7.4	7.8	9.4	10.4
- igneous	11.0	1.2	3.2	0.8	6.8	3.0	6.2
- unknown	1.2	0.0	2.4	0.8	0.0	0.0	0.0
Mica - muscovite	0.4	4.0	3.0	2.8	0.4	1.0	1.6
- biotite	0.6	3.4	1.2	0.8	0.0	0.0	0.6
Accessory - zircon	0.2	0.2	0.2	0.2	0.8	0.4	0.0
- tourmaline	0.0	0.2	0.4	0.6	0.4	0.6	0.0
- rutile	0.2	0.2	0.2	0.2	0.2	0.2	0.2
- opaques	0.0	0.0	0.0	0.6	0.8	0.4	0.0
- garnet	0.0	0.0	0.0	0.0	0.0	0.0	0.0
- ?monazite	0.0	0.2	0.0	0.0	0.2	0.0	0.0
Matrix							
Clay	0.6	3.6	0.8	15.2	0.0	0.0	0.8
Organic matter	1.0	5.8	2.8	8.0	1.6	2.4	0.8
Authigenic minerals							
Glaucony	0.0	1.2	1.4	2.4	0.2	0.0	1.8
Chlorite - replace	2.4	1.6	3.6	1.6	0.6	0.2	0.0
- fill pores	0.0	0.0	0.0	0.0	0.0	0.0	0.0
Fe Carbonate - replace	2.2	19.8	8.6	8.0	3.0	10.6	3.6
- fill pores	0.0	0.0	2.0	0.2	2.2	0.6	1.0
Clear Carbonate - replace	3.8	7.6	6.0	2.6	4.0	6.4	2.4
- fill pores	2.2	0.0	1.6	0.8	1.0	1.4	1.4
Quartz	1.0	0.0	0.0	0.0	2.2	2.8	1.0
Illite - replace	0.0	0.2	0.0	0.2	0.0	0.8	0.0
Kaolin - replace	3.0	0.6	0.0	2.8	7.2	4.6	6.4
- fill pores	0.6	0.0	0.0	1.0	5.8	2.0	3.6
Oxide	0.0	0.0	0.0	0.4	0.0	0.0	0.0
Pyrite - replace	0.0	0.0	0.0	0.0	0.0	0.2	1.6
- fill pores	0.0	0.0	0.0	0.2	0.0	0.0	0.4
Porosity							
Intergranular	0.0	2.0	0.4	0.2	1.6	1.2	1.0
Dissolution	6.4	6.6	8.8	3.6	5.6	7.6	5.4
Shrinkage	0.0	0.0	0.0	0.0	0.0	0.0	0.0
Micropores	0.2	0.2	0.0	0.2	1.0	0.4	0.8
TOTAL	100.0	100.0	100.0	100.0	100.0	100.0	100.0

4.1 Callister-1, MSCT 3, depth 3858.0m

Rock classification: **Muddy siltstone**

Texture:

Sedimentary structures:	?ripple cross-laminated siltstone cut by burrows containing ovoid clay rich ?faecal pellets up to 1 mm diameter & clay cutans. Laminae are outlined by either detrital clay & organic matter, or fine sand
Average grain size:	medium silt (0.03mm), bimodal grain size distribution
Range in grain size:	clay to medium sand
Roundness / sphericity:	angular to subangular with low sphericity
Sorting:	poor (1.93 f)
Texture:	matrix supported
Packing / grain contacts:	moderately close / point & tangential grain contacts
Pore types:	shrinkage cracks associated with the clay cutan

Composition:

Framework grains:	monocrystalline quartz, polycrystalline quartz with either straight or sutured crystal boundaries, sericitised feldspars, fresh feldspars with albite & percline twinning up to fine sand in size, lithics of dusty chert, chalcedony, shale, micaceous schist, ?volcanics & highly altered unidentified grains, straight & bent muscovite & biotite flakes up to 0.35mm, accessory silt size zircon, opaques, tourmaline & rutile
Matrix:	stringers of crenulated & blocky opaque organic matter, brown to pale yellowish brown anhedral detrital clay rims grains & fills pores, laminated orangey-brown clay filling a cutan within the burrow
Authigenic minerals:	very pale green very fine sand size grains of glaucony with wormy texture typical of glauconite, fine sand size oxidised (?goethite) grains, isolated silt to very fine sand size grains replaced by fibrous green chlorite, clear carbonate spar & dusty anhedral micrite has partially to completely replaced selected grains

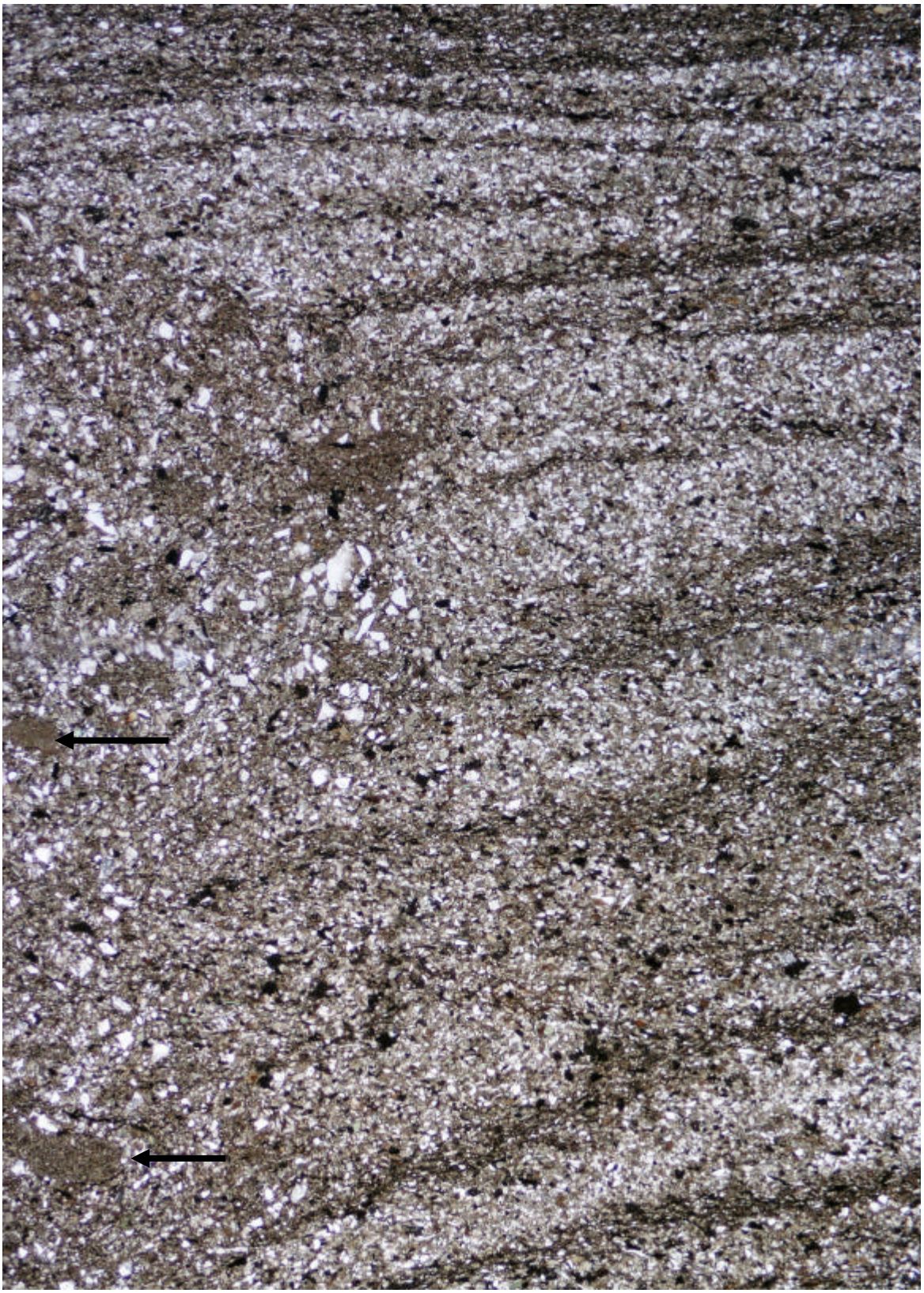

Figure 1
General field of view illustrating the contact between laminated siltstone (RHS) and a burrow. Note the disrupted texture within the burrow & possible presence of faecal pellets (arrows). Callister-1, MSCT 3, depth 3858.0m. Plane light. Horizontal field of view 6.5mm.

4.2 Callister-1, MSCT 4, depth 3849.5m

Rock classification: **Feldspathic litharenite**

Texture:

Sedimentary structures:	none apparent
Average grain size:	fine sand (0.21mm)
Range in grain size:	clay to medium sand
Roundness / sphericity:	angular to subangular with low sphericity
Sorting:	moderate (0.81 f)
Texture:	grain supported
Packing / grain contacts:	moderately close/ tangential & concavo-convex grain contacts
Pore types:	grain size dissolution pores, honeycomb pores, intragranular pores where grains have been dissolved in lithics, intergranular pores, micropores associated with chlorite rims

Composition:

Framework grains: monocrystalline quartz, polycrystalline quartz with straight crystal boundaries & dusty polycrystalline quartz with sutured crystal boundaries, fresh & corroded feldspars with albite & simple twinning, rare zoned feldspars & others with granophyric texture, sericitised feldspars lack twinning, lithics of chert, chalcedony, silty dark brown mudstone, ?granite (intergrowths of quartz & feldspar), micaceous schist, shale, quartzite, chloritised quartzite, devitrified glass, volcanics with trachytic textures & highly altered unidentified grains, highly deformed & altered mica flakes up to 0.45mm in length, accessory fine sand size rutile & very fine sand size zircon, opaques & tourmaline

Matrix: trace amounts of anhedral dark brown clay have a patchy distribution & rare blocky organic matter

Authigenic minerals: highly deformed pale yellow fine sand size grains of glaucony with wormy texture typical of glauconite, chlorite platelets oriented at right angles to grain surfaces form rims up to 10 microns thick on intergranular pores, where pores are small chlorite fills the pore, chlorite rims remain suspended where grains have been dissolved & are absent at grain contacts, rare grains have been completely replaced by fibrous green chlorite, pore filling clear carbonate spar postdates the chlorite, similar spar has partially replaced feldspars, rare highly deformed oxidised grains

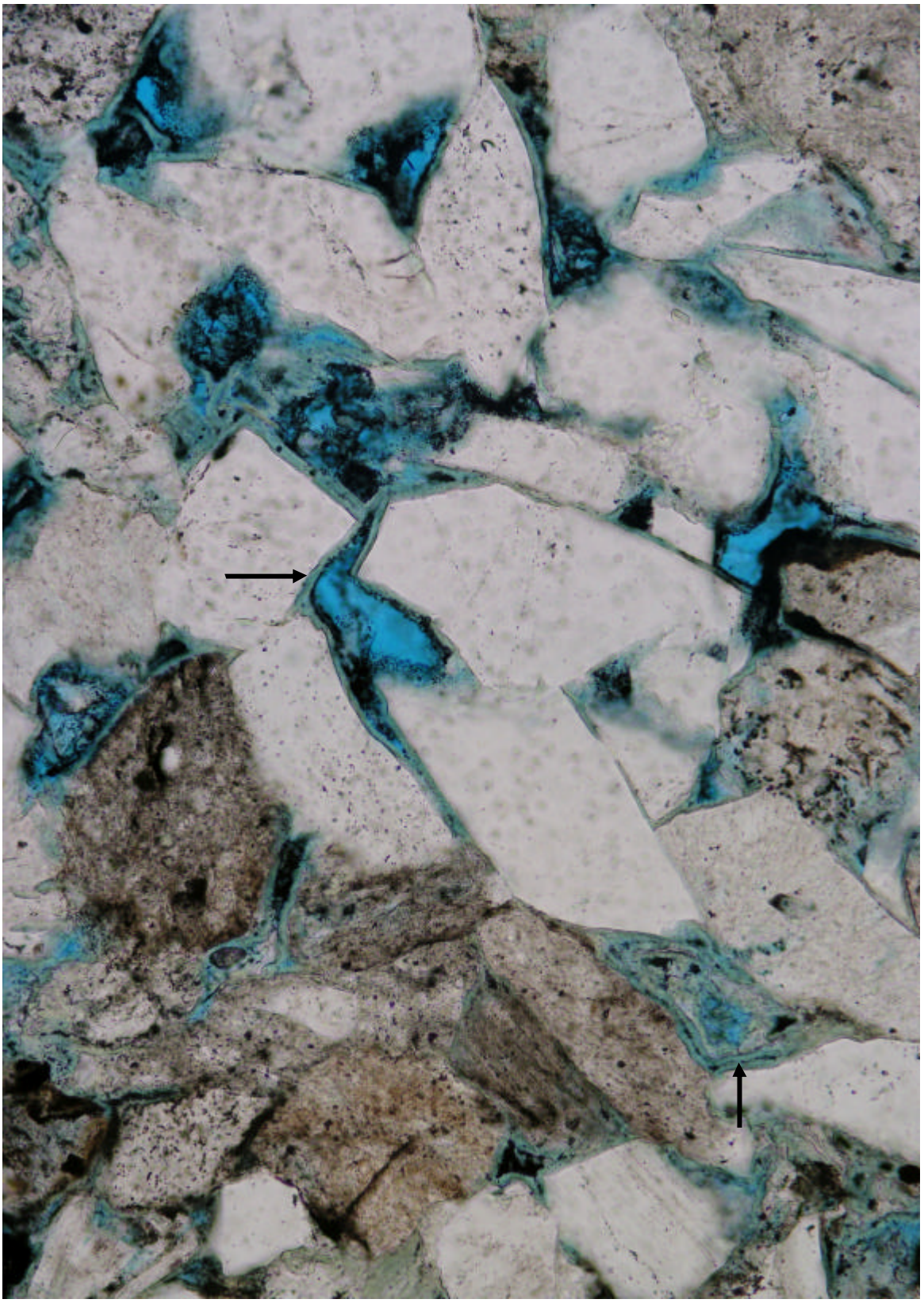

Figure 2

Intergranular pores are better preserved in those areas where there are less lithics and more detrital quartz grains. Lithics tend to deform and therefore fill adjacent intergranular pores. Note the well preserved chlorite rims (arrows) on intergranular pores. Grinding paste (opaque) is trapped in the chlorite. Callister-1, MSCT 4, depth 3849.5m. Plane light. Horizontal field of view 0.65mm.

4.3 Callister-1, MSCT 5, depth 3809.5m

Rock classification: **Feldspathic Litharenite**

Texture:

Sedimentary structures:	none apparent, sample was fragmented during sampling
Average grain size:	fine sand (0.22mm)
Range in grain size:	very fine to medium sand
Roundness / sphericity:	angular to subrounded with low to moderate sphericity
Sorting:	well (0.40 f)
Texture:	grain supported
Packing / grain contacts:	moderately close / tangential & concavo-convex grain contacts
Pore types:	primary intergranular pores, grain size dissolution pores, honeycomb pores, intragranular pores where feldspar laths have been corroded within lithics, micropores associated with chlorite rims

Composition:

Framework grains: monocrystalline quartz, polycrystalline quartz with sutured crystal boundaries, fresh & altered (sericitised & corroded) feldspars with albite & simple twinning, lithics of chert, chalcedony, silty dark brown mudstone, shale, micaceous schist, quartzite, ?pyrophyllite, chloritic quartzite, volcanics with trachytic textures, devitrified glass & highly altered unidentified grains, bent muscovite & biotite flakes up to 0.35mm in length, accessory silt size zircon & garnet

Authigenic minerals: isolated patches of pore filling & grain replacing clear carbonate spar, chlorite rims formed prior to the carbonate, typically rims are 5-10 microns thick & comprised of platelets oriented perpendicular to the grain surface, fibrous chlorite has replaced grains of unknown origin, rare prismatic quartz overgrowths

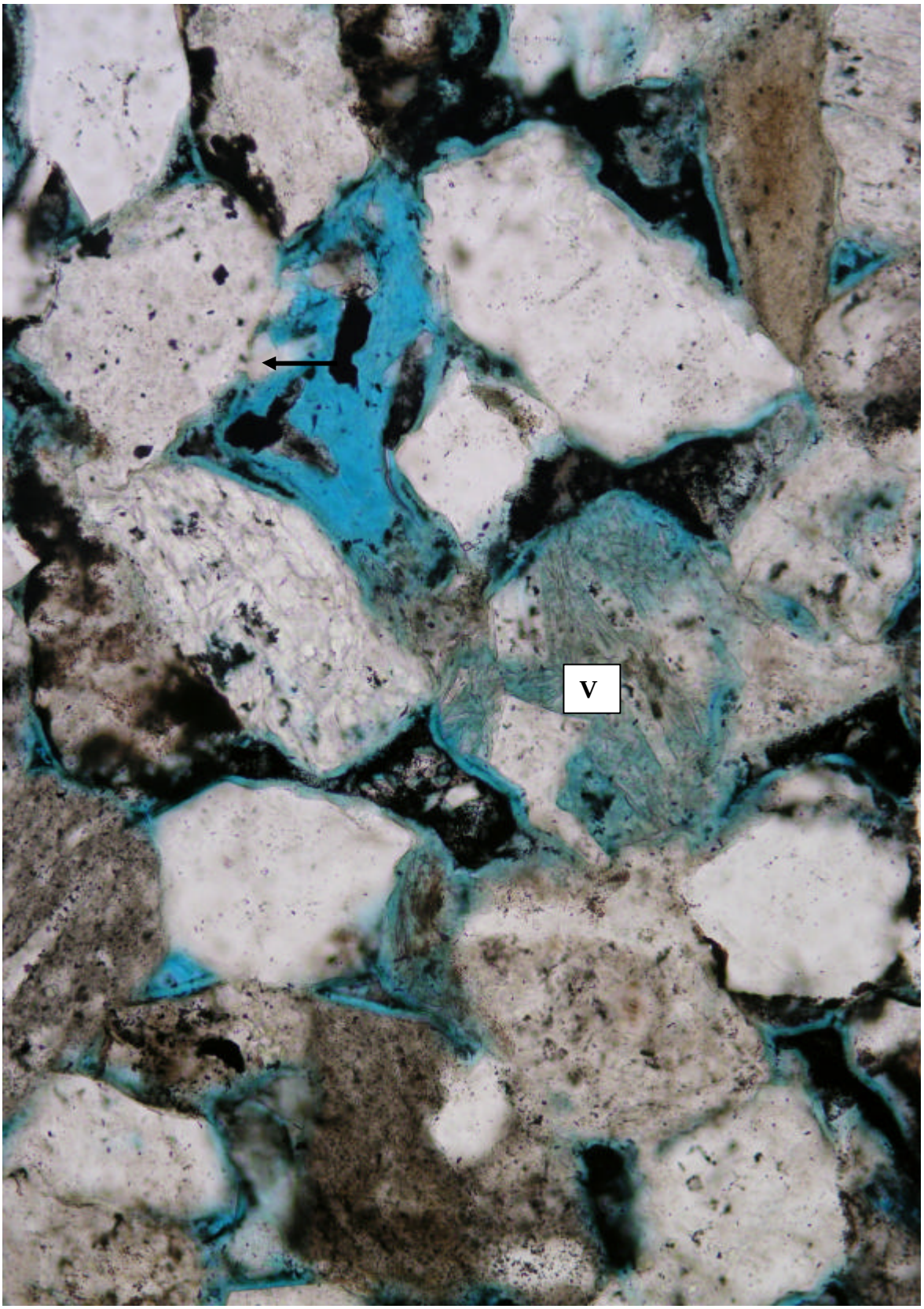

Figure 3

Intergranular pores are filled with grinding paste and drilling mud. Note the highly corroded nature of a volcanic lithic (V) and rare prismatic quartz overgrowths (arrow) adjacent to a dissolution pore. Callister-1, MSCT 5, depth 3809.5m. Plane light. Horizontal field of view 0.65mm.

4.4 Callister-1, MSCT 6, depth 3802.0m

Rock classification: **Litharenite**

Texture:

Sedimentary structures:	planar laminae outlined by changes in grain size & abundance of organic matter, laminae are less than 3mm thick
Average grain size:	medium sand (0.32mm)
Range in grain size:	fine to coarse sand
Roundness / sphericity:	angular to subangular with low sphericity
Sorting:	well (0.50 f)
Texture:	grain supported
Packing / grain contacts:	close packing/ tangential & concavo-convex contacts
Pore types:	intergranular pores, grain size dissolution pores, honeycomb pores, intragranular pores within lithics, micropores associated with kaolin & chlorite

Composition:

Framework grains: monocrystalline quartz, dusty, polycrystalline quartz with either straight or sutured crystal boundaries, sericitised & corroded feldspars, relatively fresh feldspars with albite & pericline twinning, lithics of chert, chalcedony, shale, illitic sandstone, siltstone, dark brown mudstone, chloritic quartzite, quartzite, micaceous schist, ?pyrophyllite, ?spherulitic rhyolite, volcanics with trachytic textures, devitrified glass & highly altered unidentified grains, bent flakes of biotite & straight muscovite up to 0.6mm in length, accessory silt size zircon & very fine sand size garnet

Matrix: blocky opaque organic matter

Authigenic minerals: deformed medium grain size slightly oxidised grains with remnants of wormy texture typical of glaucony, intergranular pores are rimmed by chlorite, rims tend to be 5 microns in thickness & comprised of platelets oriented perpendicular to the grain surface, chlorite rims are absent at grain contacts, rare grains completely replaced by fibrous green chlorite, pore filling & grain replacing clear carbonate spar postdates the chlorite, grain replacing & pore filling anhedral kaolin booklets up to 15 microns diameter also postdate the chlorite, traces of illite associated with selected patches of kaolin, rare prismatic quartz overgrowths

Figure 4
The planar contact between laminae in this litharenite is sharp and outlined by a change in grain size and organic matter (opaque). Note the high percentage of lithics and altered feldspars (various shades of brown). Callister-1, MSCT 6, depth 3802.0m. Plane light. Horizontal field of view 6.5mm.

4.5 Callister-1, MSCT 7, depth 3791.0m

Rock classification: **Litharenite**

Texture:

Sedimentary structures:	weak grain alignment may indicate the orientation of bedding, sample was fragmented into chips during sampling
Average grain size:	fine sand (0.20mm)
Range in grain size:	clay to medium sand
Roundness / sphericity:	angular to subangular with low sphericity
Sorting:	moderately (0.77 f)
Texture:	grain supported
Packing / grain contacts:	moderately close / tangential & concavo-convex contacts
Pore types:	primary intergranular pores, grain size dissolution pores, intragranular pores within lithics, micropores associated with chlorite & kaolin

Composition:

Framework grains: monocrystalline quartz, polycrystalline quartz with straight crystal boundaries, relatively fresh & corroded feldspars with simple & albite twinning, sericitised feldspars lack twinning, altered lithics of chert, chalcedony, dark brown mudstone, micaceous schist, shale, quartzite, ?pyrophyllite, ?granite, various volcanics including examples with trachytic texture & devitrified glass & highly altered unidentified grains, highly altered biotite & muscovite flakes up to 0.45mm in length, accessory silt size zircon

Matrix: blocky opaque organic matter associated with trace amounts of brown anhedral clay

Authigenic minerals: rare fine sand size bright green grains of glaucony, chlorite platelets oriented at right angles to grain surfaces form rims up to 5 microns thick on intergranular pores, in places these rims appear to have been oxidised, fibrous green chlorite has replaced selected grains, minor clear poikilotopic carbonate spar has filled the remaining pore space & partially replaced grains, rare prismatic quartz overgrowths formed after chlorite rims & minute pore filling & grain replacing kaolin booklets up to 5 microns diameter

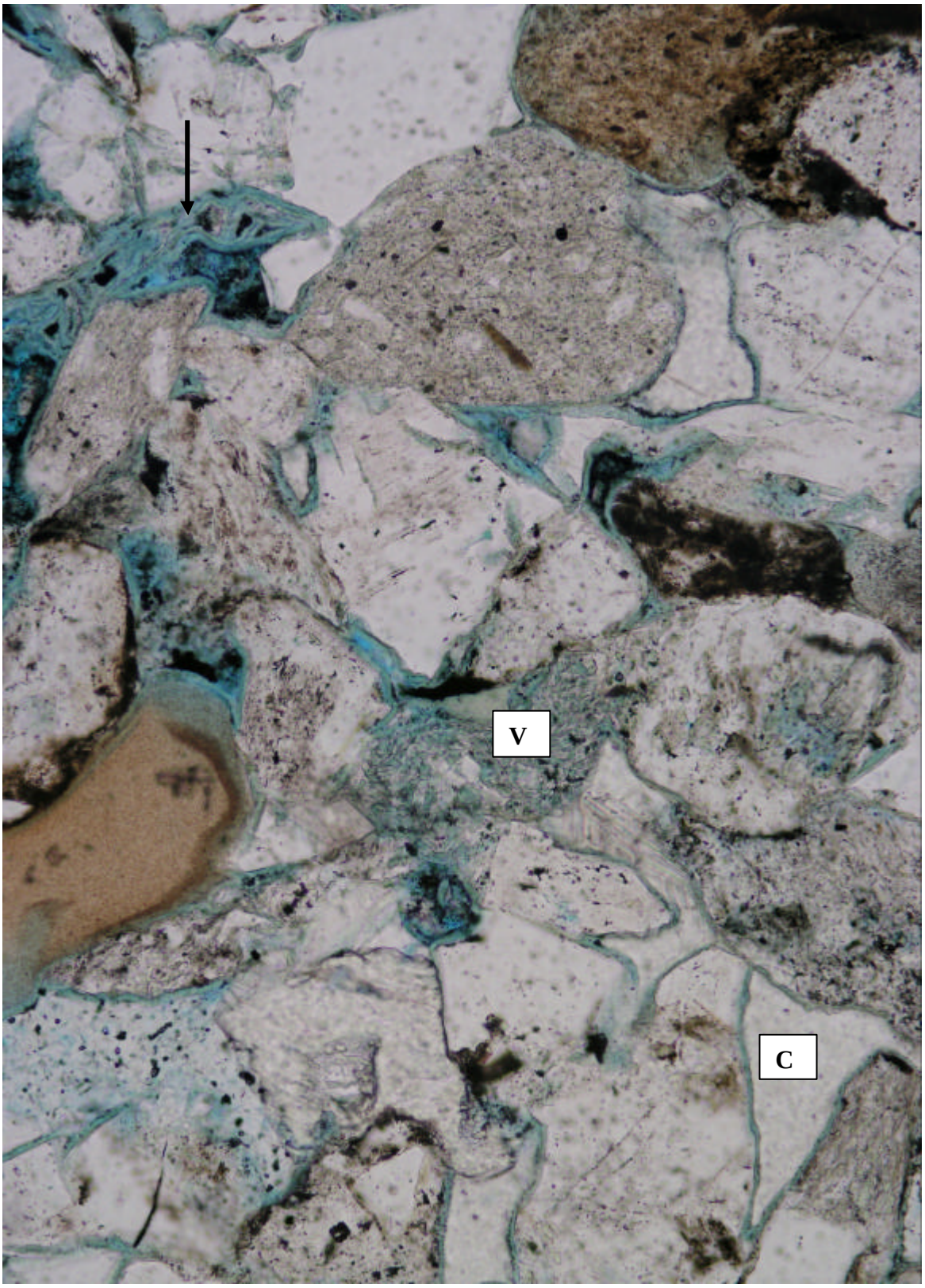

Figure 5

Chlorite rims have been deformed (arrow) where grains were dissolved prior to mechanical compaction. Note that chlorite rims are preserved around those pores filled with clear carbonate spar (C). Chlorite has also replaced the groundmass of selected volcanic lithics (V). Callister-1, MSCT 7, depth 3791.0m. Plane light. Horizontal field of view 0.65mm.

4.6 Callister-1, MSCT 9, depth 3700.0m

Rock classification: **Litharenite**

Texture:

Sedimentary structures: possible horizontal burrow filled with cleaner sand
Average grain size: fine sand (0.20mm)
Range in grain size: clay to medium sand
Roundness / sphericity: subangular with low sphericity
Sorting: moderately (0.79 f)
Texture: grain supported
Packing / grain contacts: close / concavo-convex contacts dominant, minor tangential
Pore types: remnants of intergranular pores, intragranular pores within lithics, shrinkage cracks associated with clay rich lithics, ?micropores associated with kaolin

Composition:

Framework grains: monocrystalline quartz, polycrystalline quartz with sutured crystal boundaries, relatively fresh feldspars with albite twinning, sericitised feldspars lack twinning, lithics of chert, dark brown mudstone, shale, quartzite, ?pyrophyllite, volcanics with trachytic textures, devitrified glass, ?granite (intergrowths of quartz & feldspar) & many lithics which are altered beyond recognition, bent & highly altered biotite, fresh muscovite up to 0.15mm in length, accessory silt size zircon & very fine sand size opaques & tourmaline

Matrix: blocky opaque organic matter

Authigenic minerals: fine sand size deformed grains with wormy texture typical of glaucony range in colour from white to yellowish-brown, incipient yellowish green to pale brown chlorite rims are up to 5 microns thick but do not have a uniform distribution nor do they completely rim intergranular pores, rims are absent where detrital clay is present & elsewhere partially oxidised, chlorite has selectively replaced the groundmass of some volcanic lithics & replaced mica flakes & other grains of unknown origin, clear carbonate spar has partially replaced grains & filled intergranular pores, grain replacing & pore filling anhedral kaolin booklets less than 5 microns in diameter, pyrite framboids less than 5 microns diameter replacing grains & scattered along grain margins

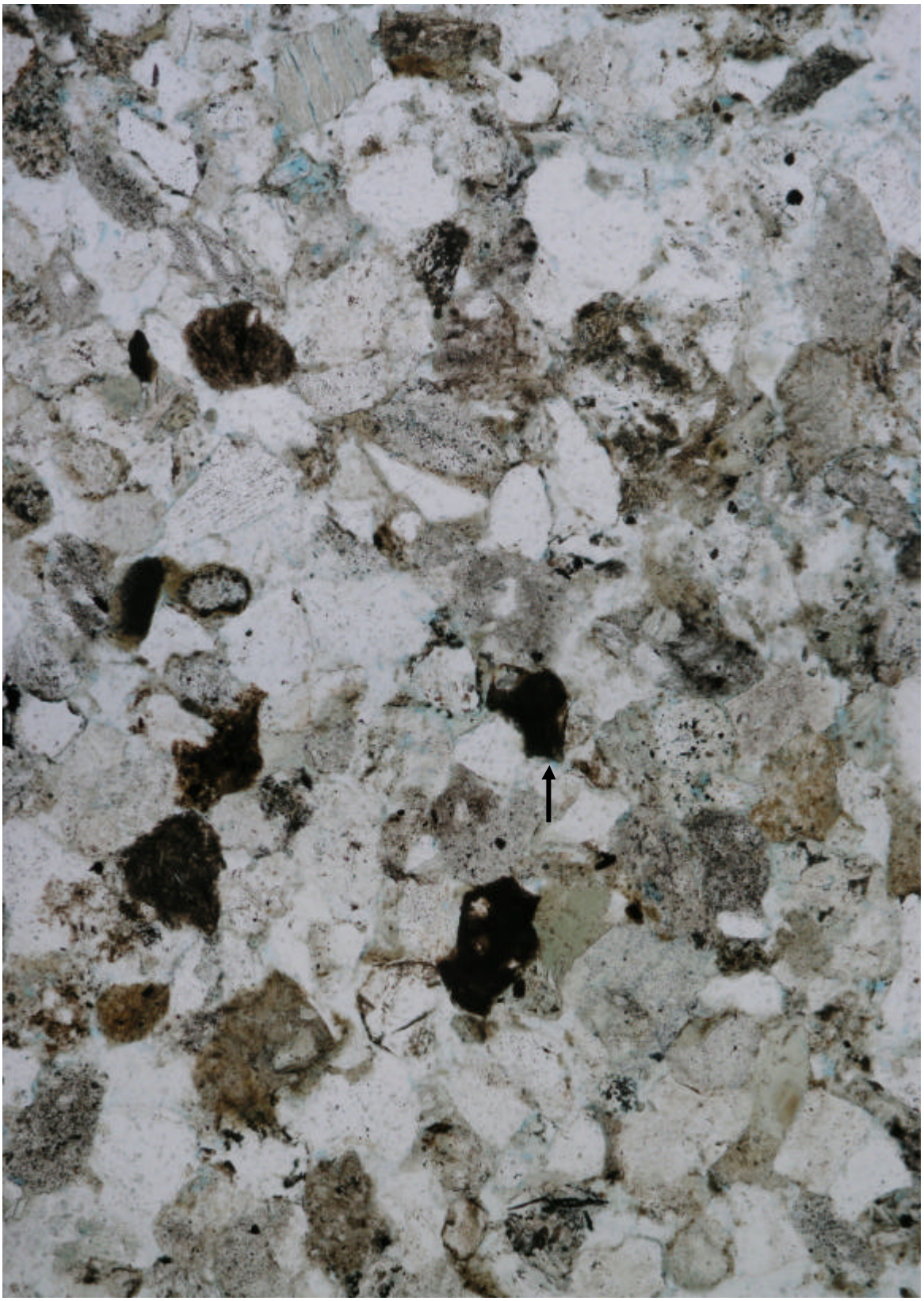

Figure 6
Typical field of view illustrating the close packing and highly altered nature of grains within this litharenite. Only remnants of intergranular pores (arrow) are apparent and these may be secondary in nature. Callister-1, MSCT 9, depth 3700.0m. Plane light. Horizontal field of view 1.30mm.

4.7 Callister-1, MSCT 10, depth 3695.5m

Rock classification: **Litharenite**

Texture:

Sedimentary structures: bedding is apparent from the presence of crenulated stringers of organic matter & alignment of up to pebble size silty mudstone/muddy siltstone lithics
Average grain size: medium sand (0.35mm)
Range in grain size: very fine sand to pebbles
Roundness / sphericity: angular to subangular with low sphericity
Sorting: moderate (0.71 f)
Texture: grain supported
Packing / grain contacts: moderately close / tangential, concavo-convex & sutured contacts
Pore types: rare intergranular pores, grain size dissolution pores, honeycomb & intragranular pores, micropores associated with kaolin

Composition:

Framework grains: monocrystalline quartz, polycrystalline quartz with either straight or sutured crystal boundaries, relatively fresh feldspars with albite & pericline twinning, sericitised feldspars either lack twinning or have albite twinning, lithics of chert, dark brown mudstone, deformed silty brown mudstone/muddy siltstone up to pebble size, shale, ?pyrophyllite, quartzite, ?spherulitic rhyolite, ?granite, corroded volcanics with trachytic texture, devitrified glass & unidentified metasediments, bent muscovite & biotite flakes up to 0.35mm in length, accessory fine sand size ?monazite & very fine sand size tourmaline & zircon
Matrix: stringers of crenulated opaque organic matter & brown anhedral clay
Authigenic minerals: colourless grains with wormy texture typical of immature glaucony, pore filling & grain replacing clear carbonate spar, grain replacing Fe rich anhedral carbonate spar & micrite appears to have been partially corroded, discontinuous incipient chlorite rims less than 5 microns thick are more common on lithics, isolated grains replaced by fibrous chlorite, straight grain contacts & rare dust rims indicate the presence of quartz overgrowths between adjacent grains of monocrystalline quartz, quartz overgrowths appear to have formed prior to the carbonate spar, pore filling & grain replacing anhedral kaolin booklets less than 5 microns diameter

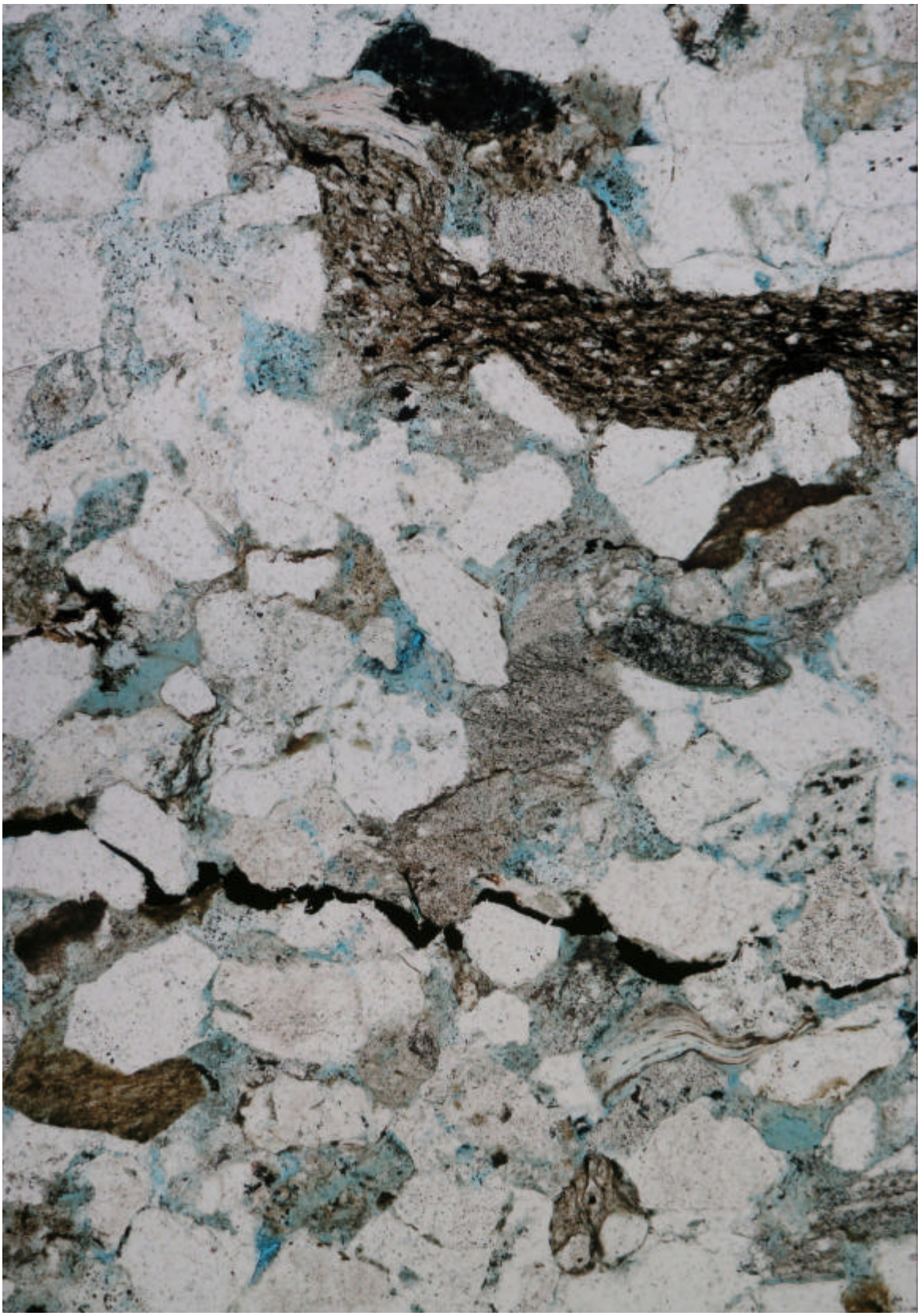

Figure 7
Alignment of the crenulated stringer of opaque organic matter and the deformed silty mudstone/muddy siltstone lithic (dark brown) indicate the orientation of bedding. Porosity (blue) is dominantly secondary in nature. Callister-1, MSCT 10, depth 3695.5m. Plane light. Horizontal field of view 1.30mm.

4.8 Callister-1, MSCT 11, depth 3620.0m

Rock classification: **Muddy siltstone**

Texture:

Sedimentary structures:	slightly deformed ovoid patches of mudstone up to 1.7mm diameter within the siltstone could represent faecal pellets, stringers of organic matter & detrital clay indicate the orientation of parallel laminae
Average grain size:	coarse silt (0.04mm), bimodal grain size distribution
Range in grain size:	clay to fine sand
Roundness / sphericity:	angular with low sphericity
Sorting:	poor (1.85 f)
Texture:	matrix supported
Packing / grain contacts:	close / concavo-convex & sutured grain contacts
Pore types:	fracturing parallel to laminae is probably the result of sampling, isolated silt size dissolution pores

Composition:

Framework grains:	monocrystalline quartz, polycrystalline quartz with either straight or sutured crystal boundaries, relatively fresh feldspars with remnants of albite twinning, other sericitised grains could also have been feldspars, lithics of dark brown mudstone, shale, quartzite, volcanic lithics with trachytic textures & devitrified glass, bent muscovite & biotite flakes up to 0.4mm in length, accessory silt size zircon, ?monazite & rutile
Matrix:	blocky opaque organic matter & crenulated stringers, pale to dark brown anhedral clay is pervasive throughout the section
Authigenic minerals:	silt size pale to dark green grains of glaucony with wormy texture, mica flakes & other grains of unknown origin replaced by dusty & clear carbonate spar, selected grains completely replaced by fibrous chlorite & the groundmass of volcanic lithics replaced by chlorite

Figure 8
Mechanical compaction has occluded porosity in this siltstone. Contact between laminae are illustrated by the presence of opaque organic matter & an increase in the dark brown clay matrix. Note the rare grain size pores (blue). Callister-1, MSCT 11, depth 3620.0m. Plane light. Horizontal field of view 1.30mm.

4.9 Callister-1, MSCT 12, depth 3614.0m

Rock classification: **Litharenite**

Texture:

Sedimentary structures:	sample was fragmented into chips during sampling, stringer of organic matter probably indicates the orientation of bedding
Average grain size:	fine sand (0.23mm)
Range in grain size:	clay to coarse sand
Roundness / sphericity:	angular to subangular with low sphericity
Sorting:	poor (1.05 f)
Texture:	grain supported
Packing / grain contacts:	close / tangential & concavo-convex contacts
Pore types:	grain size dissolution pores, intragranular pores within lithics, micropores associated with kaolin

Composition:

Framework grains: monocrystalline quartz, polycrystalline quartz with sutured or straight crystal boundaries, relatively fresh & sericitised feldspars with albite & simple twinning, rare intergrowths of quartz & alkali feldspar to produce micrographic texture, remnants of zoned feldspars, lithics of chert, chalcedony, mudstone, shale, quartzite, ?granite, ?pyrophyllite, devitrified glass, volcanics with trachytic texture & highly altered unidentified grains, straight muscovite flakes up to 0.5mm in length & bent altered biotite, accessory very fine sand size rutile & silt size zircon

Matrix: stringers & blocky opaque organic matter, dark brown clay coatings on framework grains

Authigenic minerals: dust rims outline the presence of quartz overgrowths, pore filling & grain replacing twinned poikilotopic clear carbonate spar postdates the quartz & has minor evidence of dissolution, micas replaced by irregular patches & dusty Fe rich micrite, chlorite has replaced the groundmass of selected volcanic lithics & completely replaced other grains of unknown origin, grain replacing subhedral kaolin booklets up to 15 microns diameter

Figure 9
Mechanical compaction has caused the deformation of ductile grains and resulted in close packing in this litharenite. Note the isolated grain size pore (blue) & adjacent corroded grains. Callister-1, MSCT 12, depth 3614.0m. Plane light. Horizontal field of view 1.30mm.

4.10 Callister-1, MSCT 15, depth 3535.0m

Rock classification: **Feldspathic litharenite**

Texture:

Sedimentary structures: planar laminae vary in width from two to five mm, variations in grain size & organic matter define the laminae
Average grain size: very fine sand (0.07mm)
Range in grain size: clay to fine sand
Roundness / sphericity: angular to subangular with low sphericity
Sorting: poor (1.43 f)
Texture: grain supported
Packing / grain contacts: close / tangential & concavo-convex contacts
Pore types: intergranular pores, intragranular & grain size dissolution pores concentrate in clean laminae, fracturing parallel to laminae is probably an artifact, micropores associated with kaolin

Composition:

Framework grains: monocrystalline quartz, polycrystalline quartz with sutured crystal boundaries, relatively fresh feldspars with albite twinning & rare examples with tartan twinning, other highly sericitised grains were probably feldspars, lithics of chert, chalcedony, mudstone, shale, ?granite & devitrified glass, muscovite & rare biotite flakes up to 0.45mm in length concentrate in the organic rich laminae, accessory silt size zircon, tourmaline, rutile & ?monazite
Matrix: stringers of anhedral brown clay associated with blocky cellular & crenulated opaque organic matter
Authigenic minerals: very fine sand size deformed pale yellow to green grains of glaucony with wormy texture, dusty micritic grain replacing carbonate & clear spar is concentrated in those laminae rich in organic matter, patches of micrite are up to coarse sand in size, clear spar has filled pores & replaced grains, irregular crystal boundaries suggest minor dissolution of the spar, grain replacing anhedral kaolin booklets less than 5 microns in diameter, trace amounts of illite associated with the kaolin, rare grains replaced by fibrous green chlorite

Figure 10

Coarse sand size patches of very dusty micrite are associated with organic matter (opaque), detrital clay & micas. Porosity (blue) concentrates in the intervening cleaner laminae. Note the intragranular pores (arrow) in the middle of a chalcedonic lithic. Callister-1, MSCT 15, depth 3535.0m. Plane light. Horizontal field of view 1.30mm.

4.11 Callister-1, MSCT 16, depth 3526.5m

Rock classification: **Litharenite**

Texture:

Sedimentary structures:	grain alignment indicates the orientation of bedding but there are not bed contacts apparent
Average grain size:	very fine sand (0.12mm)
Range in grain size:	clay to medium sand
Roundness / sphericity:	angular with low sphericity
Sorting:	moderately (0.98 f)
Texture:	grain supported
Packing / grain contacts:	close / tangential & concavo-convex contacts
Pore types:	rare remnants of intergranular pores, grain size dissolution pores, honeycomb & intragranular pores

Composition:

Framework grains: monocrystalline quartz, polycrystalline quartz with sutured crystal boundaries, relatively fresh feldspars with albite twinning, sericitised feldspars lack twinning, lithics of chert, abundant dark brown mudstone, micaceous schist, shale, quartzite, ?spherulitic rhyolite, ?granite, volcanics with trachytic texture, devitrified glass & other highly altered grains of unknown origin, fresh & altered muscovite & biotite flakes up to 0.25mm in length, accessory silt size rutile, tourmaline & zircon

Matrix: crenulated stringers & blocky opaque organic matter, traces of brown anhedral clay

Authigenic minerals: pale green very fine sand size grains of glaucony with wormy texture, grains replaced by fibrous green chlorite, grain replacing & pore filling dusty Fe rich micrite & anhedral microspar & clear spar, the cores of Fe rich spar have been corroded, grains of unknown origin replaced by fibrous chlorite

Figure 11
General field of view illustrating the anhedral nature of Fe rich micrite and microspar (dark brown at this magnification) & the dominance of secondary pores (blue). Callister-1, MSCT 16, depth 3526.5m. Plane light. Horizontal field of view 1.30mm.

4.12 Callister-1, MSCT 17, depth 3482.6m

Rock classification: **Siltstone**

Texture:

Sedimentary structures:	ripple cross laminae, load casts of coarser sand in muddy laminae, laminae have sharp contacts & there is evidence of grading of grain size within selected laminae
Average grain size:	coarse silt (0.04mm)
Range in grain size:	clay to medium sand
Roundness / sphericity:	angular with low sphericity
Sorting:	poor (1.79 f)
Texture:	grain supported in clean laminae & matrix supported in muddy laminae
Packing / grain contacts:	close / tangential & concavo-convex contacts
Pore types:	pores are restricted to the clean laminae where there are rare intergranular pores, secondary grain size, honeycomb & intragranular dissolution pores, & micropores associated with kaolin

Composition:

Framework grains:	monocrystalline quartz, polycrystalline quartz with straight crystal boundaries, relatively fresh & corroded feldspars with albite & simple twinning, lithics of chert, dark brown mudstone, shale, ?granite, quartzite, volcanics & other unidentified lithics, muscovite & biotite flakes up to 0.30mm in length, accessory silt size to very fine sand size tourmaline, zircon & rutile & up to fine sand size opaques concentrated in the clean laminae
Matrix:	anhedral dark brown clay & stringers of opaque organic matter concentrated in laminae up to 3mm wide in association with silt size detrital grains
Authigenic minerals:	fine sand size pale green grains of glaucony with wormy texture, highly deformed partially to completely oxidised grains of glaucony, grain replacing & pore filling subhedral kaolin booklets & verms up to 35 microns diameter, where micas have been replaced by kaolin there are traces of illite & booklets are up to 50 microns in diameter, pore filling & grain replacing clear poikilotopic carbonate spar, dusty Fe rich micrite is also grain replacing & pore filling but it concentrates in the laminae rich in organic matter & detrital clay, isolated grains replaced by fibrous green chlorite, rare pyrite framboids on grain margins

Figure 12

The orientation of micas within the muddy laminae (dark brown) indicate that the weight of the overlying sand caused curvature (load cast) at the contact between laminae. Note the high percentage of opaque grains in the clean laminae. Callister-1, MSCT 17, depth 3482.6m. Plane light. Horizontal field of view 3.25mm.

4.13 Callister-1, MSCT 18, depth 3481.0m

Rock classification: **Feldspathic litharenite**

Texture:

Sedimentary structures:	weakly defined cross lamination outlined by changes in grain size
Average grain size:	fine sand (0.22mm)
Range in grain size:	very fine to medium sand
Roundness / sphericity:	angular with low sphericity
Sorting:	well (0.46 f)
Texture:	grain supported
Packing / grain contacts:	close packing / tangential & concavo-convex contacts
Pore types:	remnants of intergranular pores, secondary grain size & honeycomb dissolution pores, micropores associated with kaolin

Composition:

Framework grains: monocrystalline quartz, polycrystalline quartz with either straight or sutured crystal boundaries, sericitised & highly corroded feldspars, relatively fresh feldspars with pericline, albite & simple twinning, lithics of chert, chalcedony, dark brown silty mudstone, siltstone, shale, micaceous schist, quartzite, ?granite & highly altered volcanics, muscovite flakes up to 0.3mm in length, accessory very fine to fine sand size zircon, ?monazite, tourmaline, rutile & opaques concentrated in the finer grained laminae

Matrix: rare crenulated stringers & blocky opaque organic matter, where organic matter appears to fill pores it could be reservoir bitumen

Authigenic minerals: fine sand size white to pale green grains with wormy texture typical of glaucony, euhedral quartz overgrowths have a jagged contact with grain replacing & pore filling kaolin booklets, booklets are commonly anhedral & up to 20 microns diameter but where micas have been replaced the booklets are significantly larger, clear euhedral spar was precipitated after corrosion of labile grains, clear spar has replaced grains & filled pores, dusty anhedral Fe rich micrite & spar has also replaced grains & filled pores after the kaolin, Fe rich spar is corroded on pore margins, rare grains replaced by fibrous chlorite

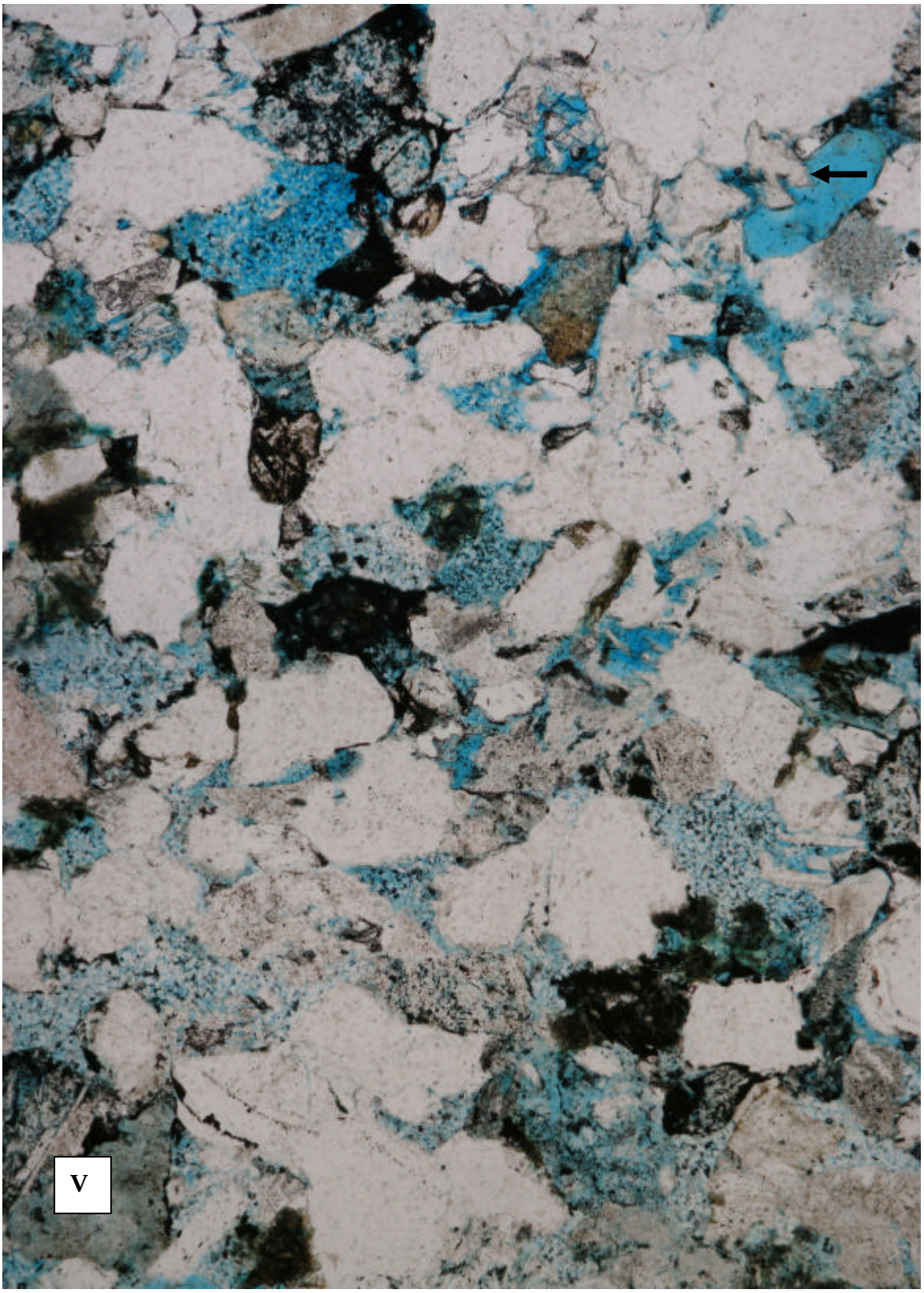

Figure 13
General field of view illustrating the abundance of grain replacing and pore filling kaolin (speckled texture) & secondary nature of porosity (blue). Note the clear carbonate spar (arrow) which formed after the dissolution of a labile grain. Dusty volcanic lithics (V) are also apparent. Callister-1, MSCT 18, depth 3481.0m. Plane light. Horizontal field of view 1.30mm.

4.14 Callister-1, MSCT 20, depth 3471.0m

Rock classification: **Litharenite & siltstone**

Texture:

Sedimentary structures: the sample has been disaggregated into two chips of differing lithology (sandstone & siltstone) but there is no evidence of a contact between the rock types, bedding is apparent within the siltstone

Average grain size: medium sand (0.35mm) & coarse silt (0.06mm)

Range in grain size: medium silt to coarse sand

Roundness / sphericity: subangular to subrounded with low to moderate sphericity in the sandstone, angular with low sphericity in the siltstone

Sorting: poor (1.41 f)

Texture: grain supported

Packing / grain contacts: moderately close packing in sandstone with dominantly tangential grain contacts, close packing in the siltstone

Pore types: in the sandstone there are primary intergranular pores, grain size, intragranular & honeycomb dissolution pores & micropores associated with kaolin, in the siltstone there are rare grain size & intragranular pores

Composition:

Framework grains: in the sandstone – monocrystalline quartz, polycrystalline quartz with either straight or sutured crystal boundaries, sericitised & corroded feldspars with remnants of albite twinning, lithics of chert, chalcedony, siltstone, micaceous schist, quartzite, shale, ?pyrophyllite, ?granite & altered volcanics, accessory fine sand size rutile & opaques

in the siltstone – monocrystalline quartz, polycrystalline quartz with sutured crystal boundaries, relatively fresh feldspars with albite twinning, lithics of chert, quartzite, shale & altered volcanics, straight & bent muscovite flakes up to 0.10mm in length, accessory very fine sand size tourmaline & silt size zircon, rutile, tourmaline & opaques

Matrix: in the siltstone - fragmented opaque & reddish & rare cellular organic matter concentrates in one laminae

Authigenic minerals: in the sandstone – euhedral quartz overgrowths are outlined by distinct dust rims & have a jagged contact with grain replacing & pore filling kaolin booklets, the latter are typically subhedral & 15 microns diameter, pore filling & grain replacing clear subhedral spar postdates the kaolin, quartz & a phase of grain replacing dusty anhedral Fe rich micrite, Fe rich micrite & spar has partially replaced grains & filled pores, clear spar appears partially corroded

in the siltstone – rounded nodules of dusty anhedral Fe rich micrite/microspar up to 0.3mm diameter are concentrated in the laminae containing organic matter, isolated grains replaced by fibrous chlorite, clear rhombs of carbonate spar appear to postdate the micrite, micas replaced by kaolin & traces of illite, rare pyrite framboids replace lithics

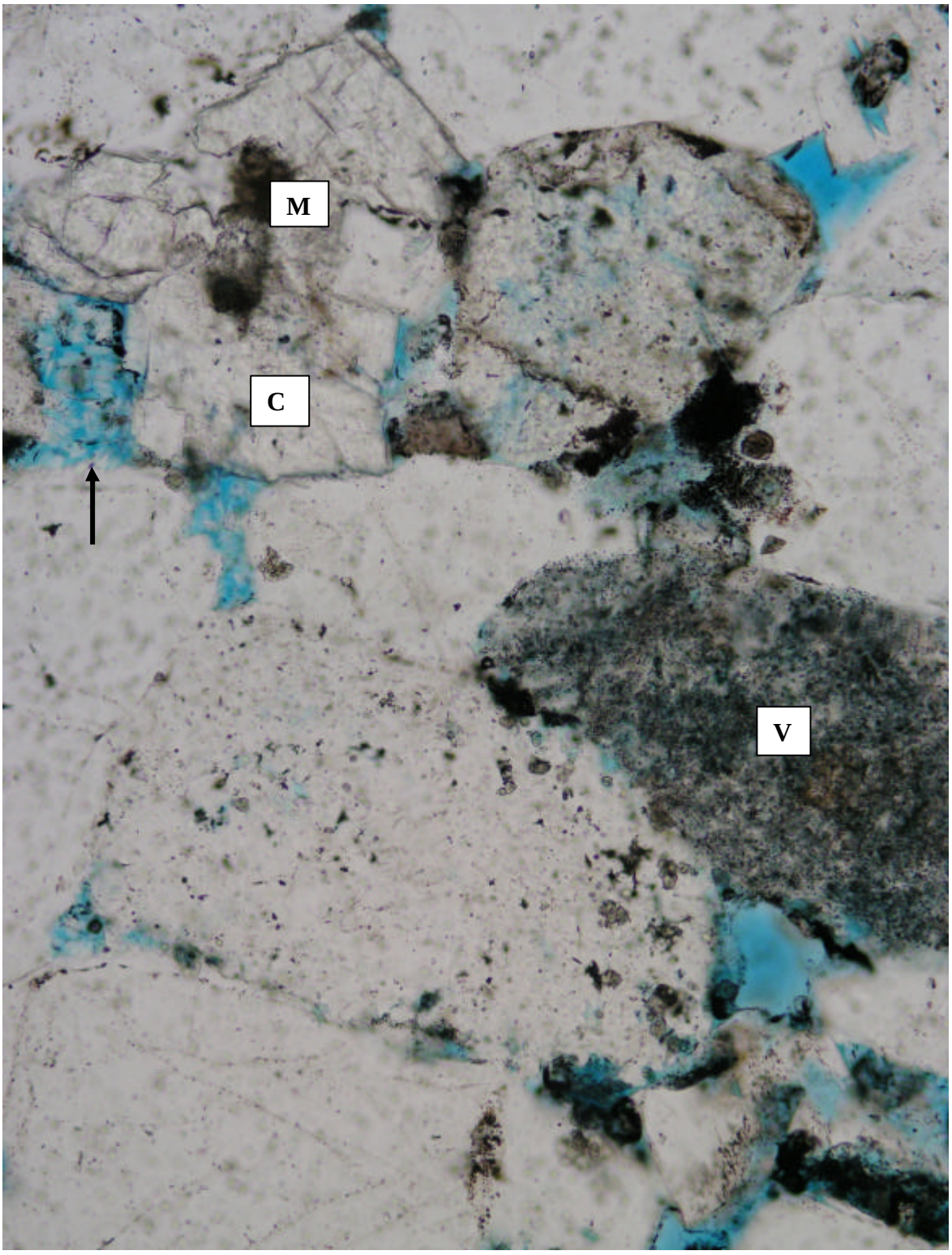

Figure 14a

Sandstone cement stratigraphy is evident in this field of view. Dusty micrite (M) formed prior to clear carbonate spar (C). Spar formed after kaolin booklets which have a jagged contact (arrow) with quartz overgrowths. Adjacent to the clear spar is a sericitised feldspar and below this is an altered volcanic (V) lithic. Callister-1, MSCT 20, depth 3471.0m. Plane light. Horizontal field of view 0.65mm.

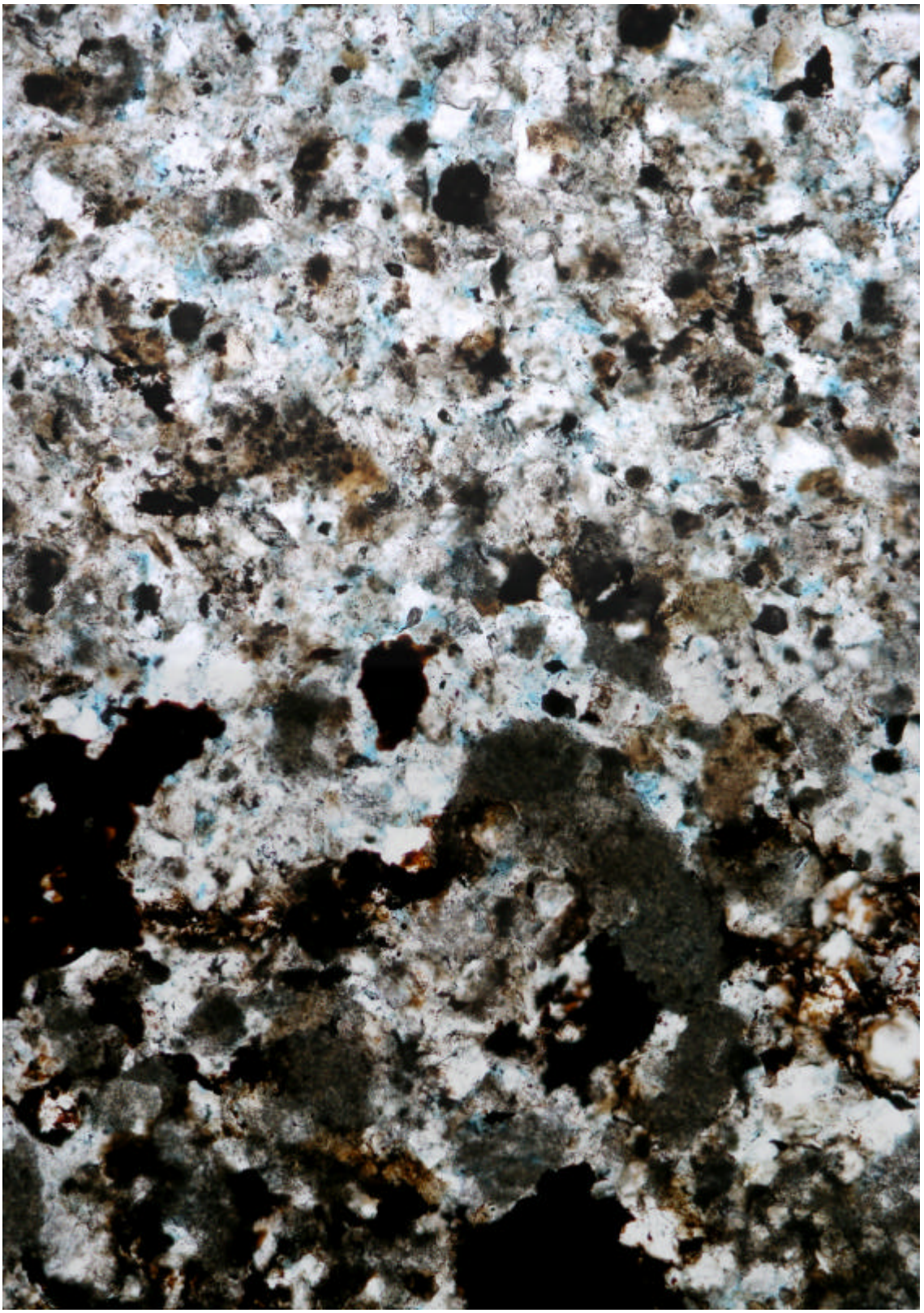

Figure 14b
Contact between these laminae in the siltstone are outlined by the variable concentration of organic matter (opaque) and micritic carbonate. Callister-1, MSCT 20, depth 3471.0m. Plane light. Horizontal field of view 1.30mm.

4.15 Callister-1, MSCT 21, depth 3464.0m

Rock classification: **Feldspathic litharenite**

Texture:

Sedimentary structures:	grain alignment & discontinuous stringers of clay & organic matter indicate the orientation of bedding
Average grain size:	fine sand (0.25mm)
Range in grain size:	clay to coarse sand
Roundness / sphericity:	angular with low sphericity
Sorting:	moderate (0.83 f)
Texture:	grain supported
Packing / grain contacts:	moderately close/ tangential & concavo-convex contacts
Pore types:	remnants of intergranular pores, grain size, honeycomb & intragranular dissolution pores & micropores associated with kaolin

Composition:

Framework grains: monocrystalline quartz, polycrystalline quartz with straight crystal boundaries, sericitised & corroded feldspars with remnants of albite twinning, rare quartz & feldspar intergrowths to produce micrographic texture, lithics of chert, chalcedony, shale, micaceous schist, quartzite, deformed mudstone, ?granite, devitrified glass & altered volcanics (including groundmass dissolved & trachytic texture remaining), straight & splayed muscovite & highly altered biotite flakes up to 0.55mm in length, accessory fine sand size rutile

Matrix: stringers of brown anhedral clay & blocky & fragmented opaque organic matter

Authigenic minerals: fine sand size rounded green grains of glaucony with wormy texture, rare prismatic quartz overgrowths, grain replacing & pore filling kaolin booklets up to 15 microns diameter, pore filling & grain replacing (feldspars) clear twinned poikilotopic carbonate spar, dusty anhedral micrite & spar replacing grains & filling pores prior to the clear spar, blocky & framboidal pyrite up to 30 microns diameter aligned along grain margins & replacing grains after the clear spar

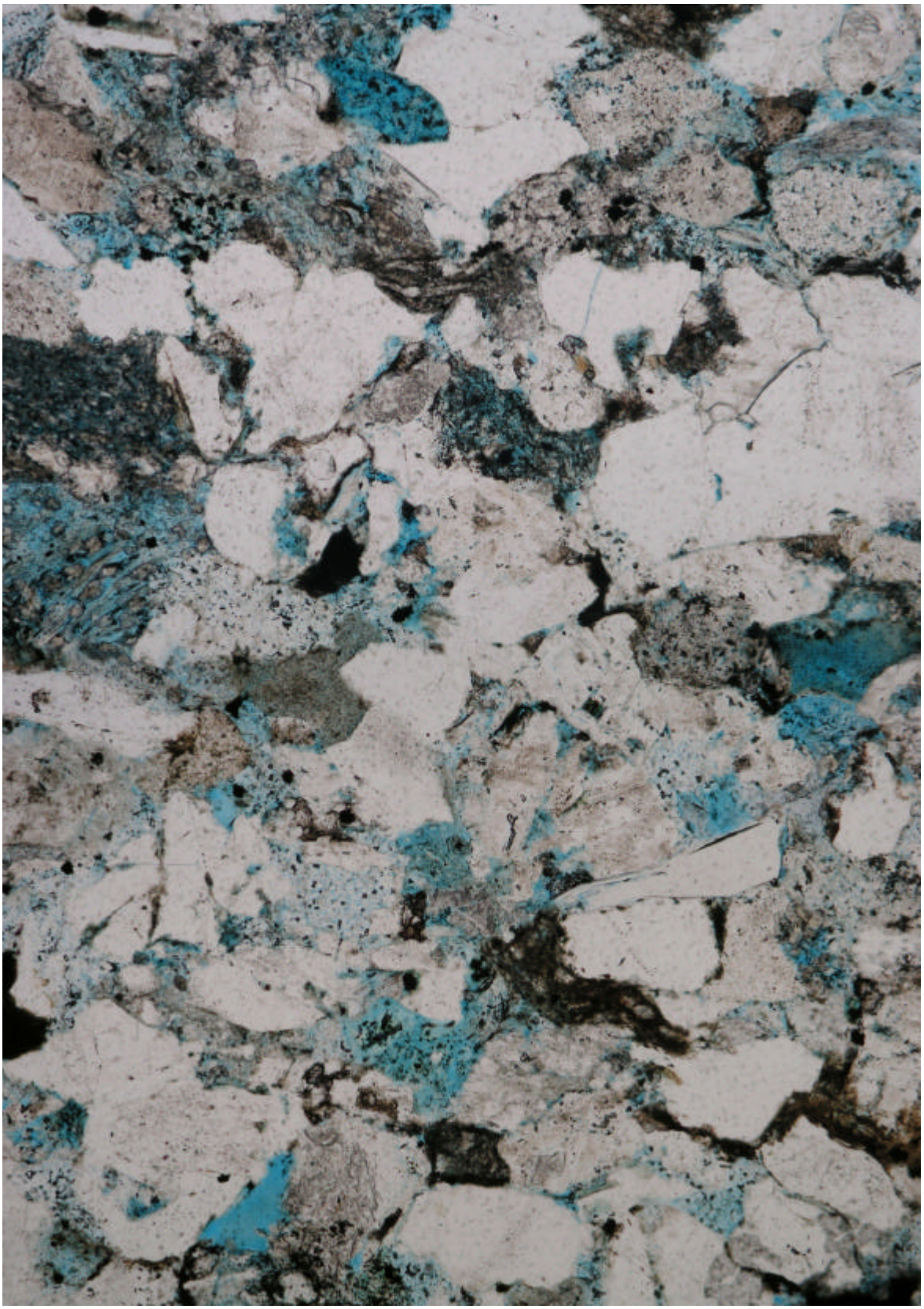

Figure 15
General field of view illustrating the dominance of grain size dissolution pores and areas of kaolin (speckled) with associated micropores. Both these pore types are unlikely to be well interconnected thus limiting permeability Callister-1, MSCT 21, depth 3464.0m. Plane light. Horizontal field of view 1.30mm.

5. GRAIN SIZE ANALYSIS

Thin Section Statistics				Frequency Distribution
MSCT:		**3**		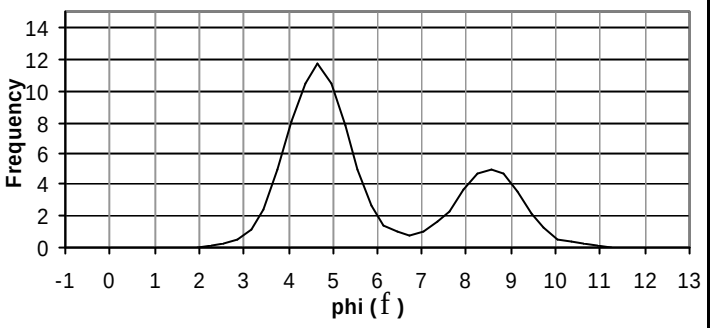
Depth (m)		**3858.00**		
Parameter		mm	ϕ	
Mean		0.03 medium silt	5.92	
Mode		0.04 coarse silt	4.65	
Range:	min	0.001	9.97	
	max	0.15	2.74	
Standard Deviation		0.02 poorly sorted	1.93	
MSCT:		**4**		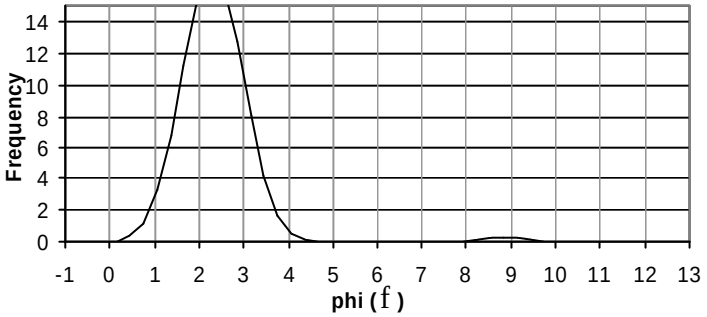
Depth (m)		**3849.50**		
Parameter		mm	ϕ	
Mean		0.21 fine sand	2.36	
Mode		0.20 fine sand	2.32	
Range:	min	0.002	8.97	
	max	0.45	1.15	
Standard Deviation		0.07 moderately sorted	0.81	
MSCT:		**5**		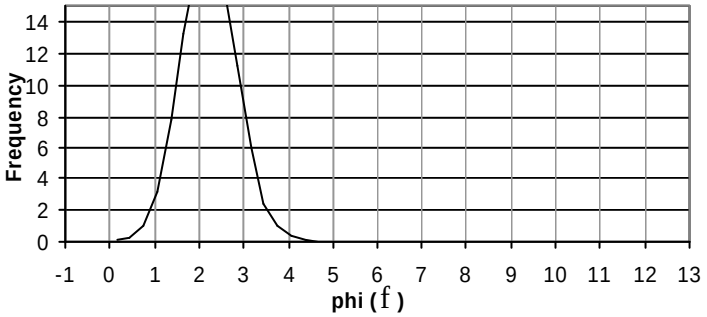
Depth (m)		**3809.50**		
Parameter		mm	ϕ	
Mean		0.22 fine sand	2.22	
Mode		0.22 fine sand	2.17	
Range:	min	0.10	3.32	
	max	0.48	1.06	
Standard Deviation		0.06 well sorted	0.40	

Thin Section Statistics				Frequency Distribution
MSCT:		**6**		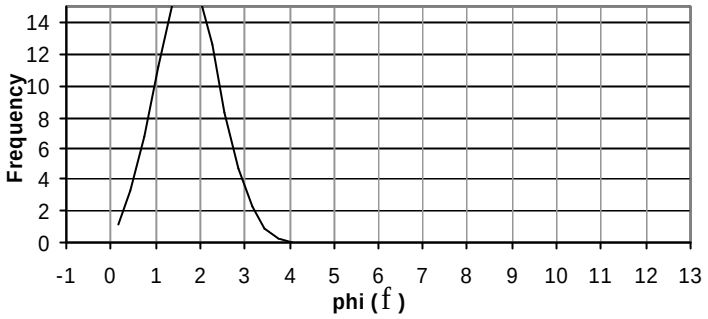
Depth (m)		**3802.00**		
Parameter		mm	ϕ	
Mean		0.32 medium sand	1.72	
Mode		0.31 medium sand	1.71	
Range:	min	0.13	2.94	
	max	0.70	0.51	
Standard Deviation		0.11 well sorted	0.50	
MSCT:		**7**		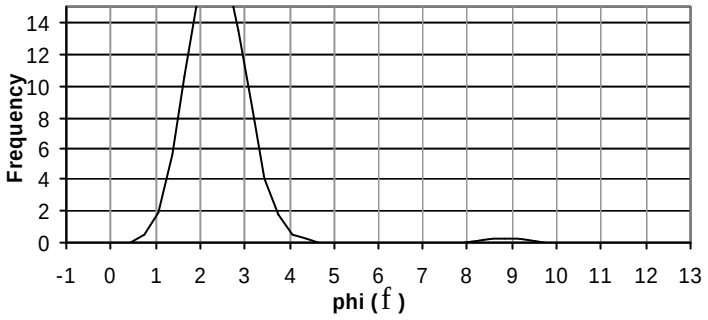
Depth (m)		**3791.00**		
Parameter		mm	ϕ	
Mean		0.20 fine sand	2.42	
Mode		0.20 fine sand	2.35	
Range:	min	0.002	8.97	
	max	0.35	1.51	
Standard Deviation		0.06 moderately sorted	0.77	
MSCT:		**9**		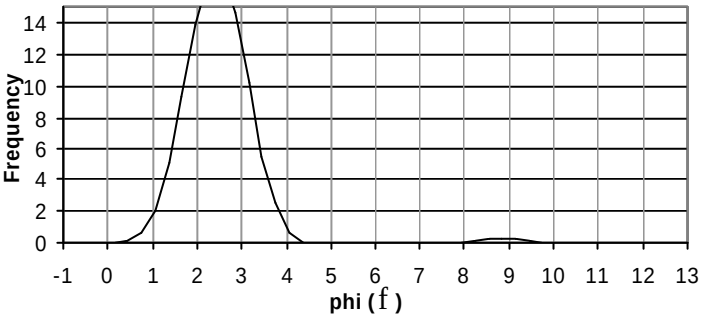
Depth (m)		**3700.00**		
Parameter		mm	ϕ	
Mean		0.20 fine sand	2.47	
Mode		0.19 fine sand	2.41	
Range:	min	0.002	8.97	
	max	0.38	1.40	
Standard Deviation		0.07 moderately sorted	0.79	
MSCT:		**10**		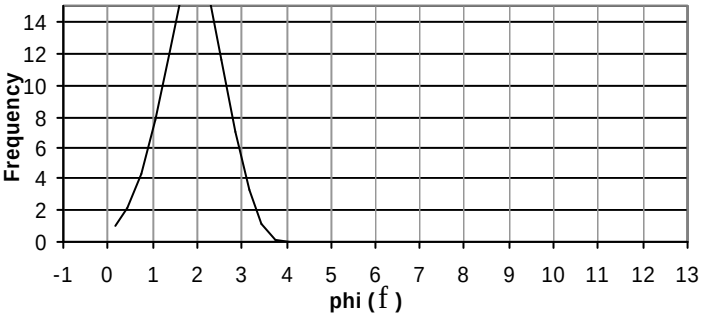
Depth (m)		**3695.50**		
Parameter		mm	ϕ	
Mean		0.35 medium sand	1.83	
Mode		0.26 medium sand	1.93	
Range:	min	0.11	3.18	
	max	4.60	-2.20	
Standard Deviation		0.52 moderately sorted	0.71	

Thin Section Statistics				Frequency Distribution
MSCT:		**11**		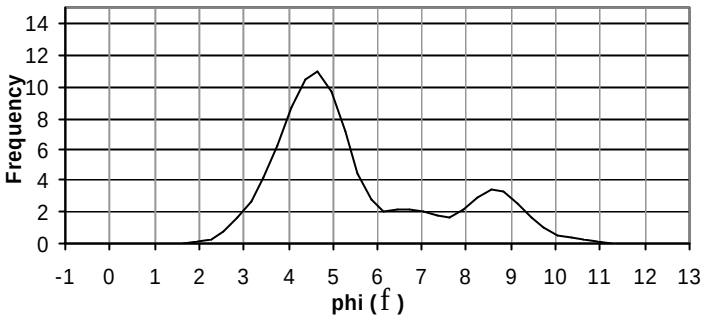
Depth (m)		**3620.00**		
Parameter		mm	ϕ	
Mean		0.04 coarse silt	5.54	
Mode		0.04 coarse silt	4.56	
Range:	min	0.001	9.97	
	max	0.15	2.74	
Standard Deviation		0.03 poorly sorted	1.85	
MSCT:		**12**		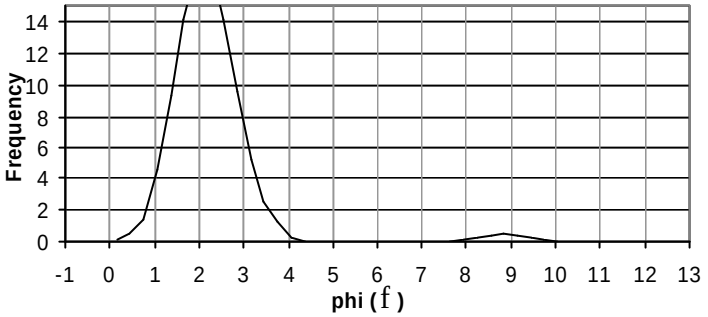
Depth (m)		**3614.00**		
Parameter		mm	ϕ	
Mean		0.23 fine sand	2.27	
Mode		0.23 fine sand	2.09	
Range:	min	0.002	8.97	
	max	0.55	0.86	
Standard Deviation		0.08 poorly sorted	1.05	
MSCT:		**15**		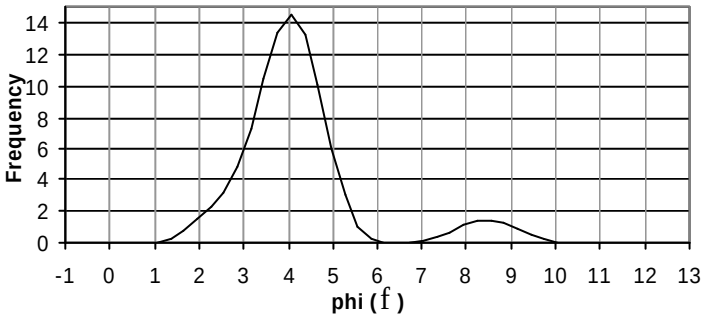
Depth (m)		**3535.00**		
Parameter		mm	ϕ	
Mean		0.07 coarse silt	4.25	
Mode		0.06 coarse silt	4.04	
Range:	min	0.002	8.97	
	max	0.21	2.25	
Standard Deviation		0.04 poorly sorted	1.43	
MSCT:		**16**		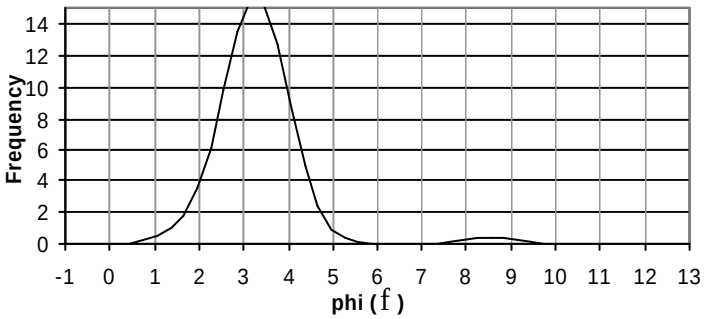
Depth (m)		**3526.50**		
Parameter		mm	ϕ	
Mean		0.12 very fine sand	3.29	
Mode		0.10 very fine sand	3.28	
Range:	min	0.002	8.97	
	max	0.41	1.29	
Standard Deviation		0.06 moderately sorted	0.98	

Thin Section Statistics				Frequency Distribution
MSCT:		**17**		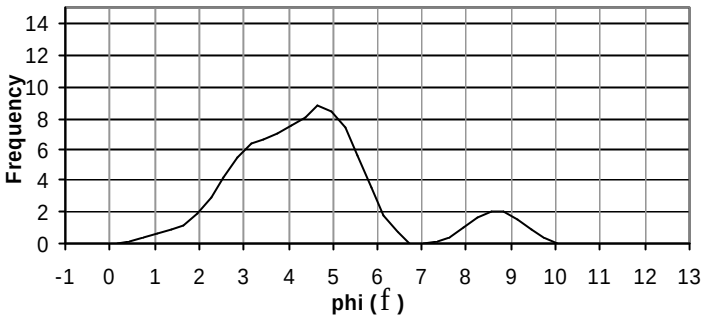
Depth (m)		**3482.60**		
Parameter		mm	ϕ	
Mean		0.07 coarse silt	4.56	
Mode		0.04 coarse silt	4.74	
Range:	min	0.002	8.97	
	max	0.43	1.22	
Standard Deviation		0.08 poorly sorted	1.79	
MSCT:		**18**		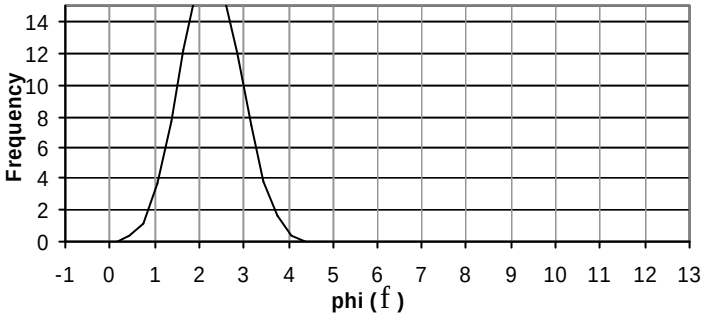
Depth (m)		**3481.00**		
Parameter		mm	ϕ	
Mean		0.22 fine sand	2.25	
Mode		0.22 fine sand	2.21	
Range:	min	0.10	3.32	
	max	0.45	1.15	
Standard Deviation		0.07 well sorted	0.46	
MSCT:		**20**		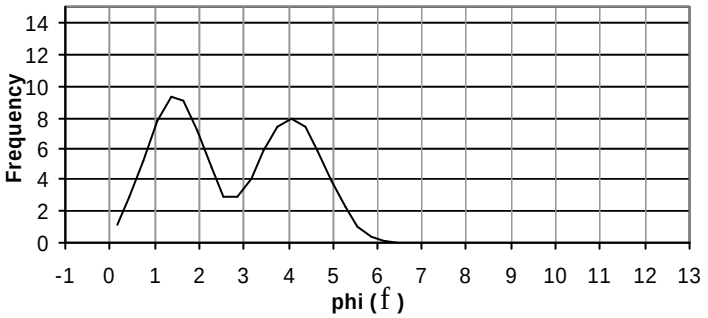
Depth (m)		**3471.00**		
Parameter		mm	ϕ	
Mean		0.23 fine sand	2.72	
Mode		0.36 medium sand	1.48	
Range:	min	0.02	5.64	
	max	0.75	0.42	
Standard Deviation		0.18 poorly sorted	1.41	
MSCT:		**21**		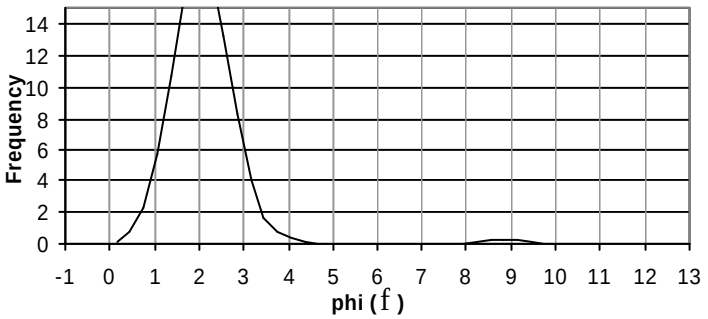
Depth (m)		**3464.00**		
Parameter		mm	ϕ	
Mean		0.25 fine sand	2.12	
Mode		0.24 fine sand	2.05	
Range:	min	0.002	8.97	
	max	0.50	1.00	
Standard Deviation		0.08 moderately sorted	0.83	

6. DISCUSSION

6.1 Lithology & texture

Samples of sandstone from Callister-1 are comprised of very fine to medium grained, poor to well sorted litharenites and feldspathic litharenites (Fig. 16). These sandstones are lithologically very similar to sediment from the Waarre A at Casino-2 (Phillips, 2003) and Casino-3 (Phillips, 2004a). Laminae and planar bedding are outlined by changes in grain size and stringers of organic matter and detrital clay. One litharenite (MSCT 9, 3700m) may have a horizontal burrow filled with clean sand. Grain shape is typically angular with low to moderate sphericity and ranges from angular to subrounded. Grain size ranges from clay to pebbles and commonly has a unimodal and symmetrical distribution.

In addition, there are three muddy siltstones that have bimodal grain size distributions at Callister-1 and one litharenite is probably interbedded with a siltstone (MSCT 20, depth 3471m). Typically the siltstones have ripple cross laminae, possible faecal pellets and a load cast in MSCT 17 (depth 3482.6m). Grain shape is more angular than the sandstones and grain size ranges from clay to medium sand.

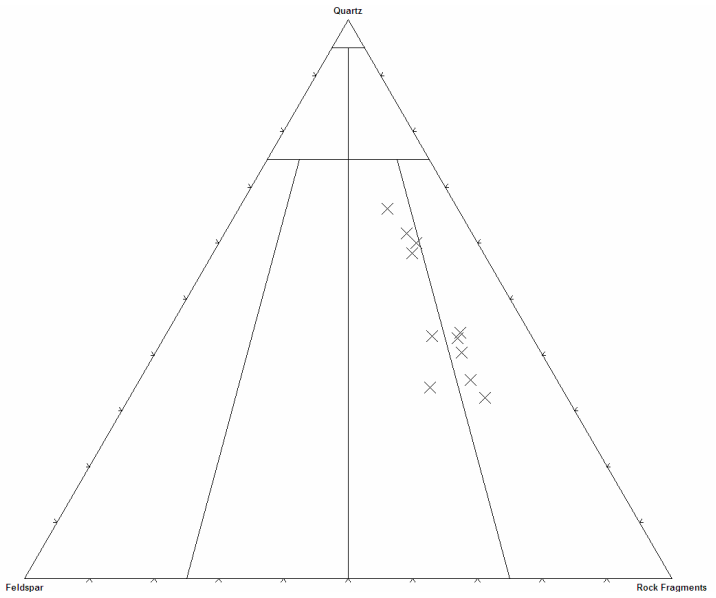

Figure 16 Folk classification for sandstones from Callister-1

6.2 Detrital mineralogy & sediment provenance

Litharenites and feldspathic litharenites at Callister-1 had a very similar sediment provenance to that described from the Casino Field and Pecten-1A (Phillips, 2004b). A metamorphic terrane was more important than the igneous source throughout deposition of these sediments. In contrast, at Martha-1 (Phillips, 2005) an igneous source was more significant and this was thought to be dominantly basic/mafic volcanics and plutonics. Volcanics and plutonics at Casino and Callister-1 are probably derived mainly from an acid/felsic igneous source.

The lithic assemblages at Callister-1 and Casino-3 are identical, but there are more lithics at Callister-1. Sedimentary lithics include chert, chalcedony, mudstone and rare siltstone. Metamorphic lithics of

shale, micaceous schist, quartzite and minor ?pyrophyllite are apparent. Igneous lithics are represented by volcanics with trachytic texture, volcanic glass, rhyolite and ?granite, and probably feldspar-quartz intergrowths to form micrographic texture. Possible granitic lithics were only noted at depths shallower than 3700m (MSCT 9) in Callister-1. It would appear that the sediment sources were relatively unchanged across the Mussel Platform. Callister-1 may have been closer to the metamorphic/igneous source than the Casino Field, thus more lithics are preserved in the sandstones.

Changes in lithic content with depth were noted for the Casino Field and very similar trends are apparent at Callister-1. The abundance of lithics decreases in shallower sandstones at Callister-1 (Fig. 17a) but this trend is not smooth, there is a break at approximately 3600 to 3550m. Below this depth lithics represent more than 28% of the total rock composition but above it lithics are less than 20% of the total rock composition. This trend is evident in both the igneous and metamorphic lithics (Fig. 17b) but not the sedimentary lithics which remain consistently at 6% or less. The significance of this break might reflect a change in tectonic activity with more uplift and/or faulting in the igneous/metamorphic terrane resulting in more lithics.

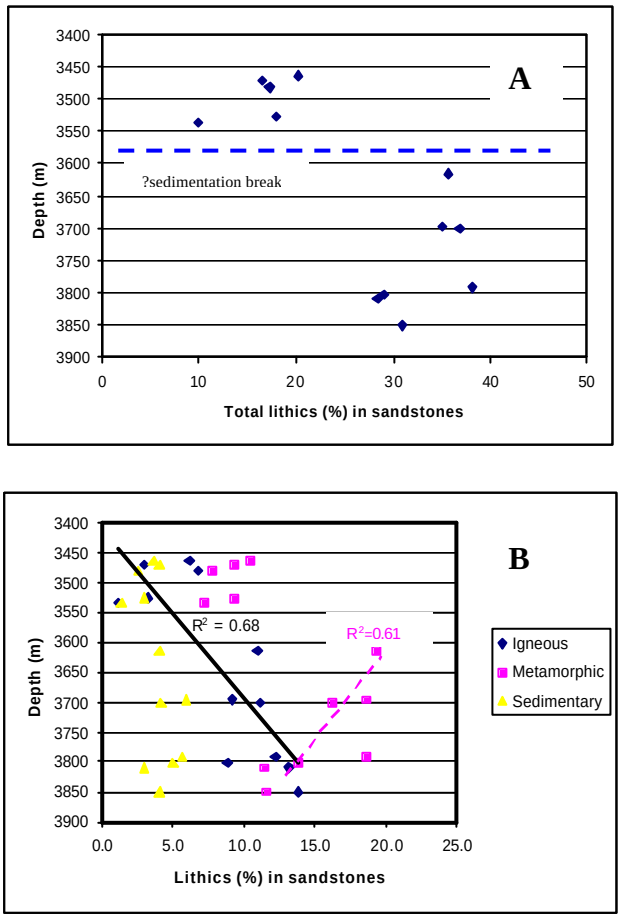

Figure 17. Relationships between depth and abundance (A)/type (B) of lithics in sandstones at Callister-1

Below the break (approximately 3600 to 3550m) the number of metamorphic lithics increases upwards from the base of the sequence ($r^2 = 0.61$) as illustrated in Figure 17b. Igneous lithics tend to follow a more continuous decline in abundance below and above the break ($r^2=0.68$). Exactly the same trends are evident in the Waarre Formation at Casino-3 (Unit A) with the break occurring at approximately 2055m. It was suggested for Casino-3 that either there was uplift in the metamorphic source or that replacement by carbonate cement had created an artificial trend. Based on the evidence from Callister-1 it is now apparent that the trends are real. Tectonic activity in the metamorphic source terrane increased and then declined during deposition of Waarre Unit A. At the igneous source there was a steady decline in tectonic activity.

Abundance and type of feldspars in the sandstones at Callister-1 follow similar trends to the lithics. There is an overall decline in feldspar content at shallower depths (r^2 = 0.60) with the change occurring at approximately 3600 to 3550m (Fig. 18a). Below this depth there are greater than 7% total feldspars and above it there are less than 7%. Plagioclase (albite) shows a continuous decline (r^2 = 0.67) as depth becomes shallower (Fig. 18b), similar to the trend in igneous lithics. This might indicate that most of the plagioclase was derived from the igneous source (granites and rhyolites). In contrast, potassium rich feldspars initially increase in abundance from the base of the sequence up to the break at approximately 3600 to 3550m following the path of metamorphic lithics. Potassium feldspars (orthoclase and microcline) can be abundant in feldspathic micaceous gneisses and schists and quartzites. Therefore it is consistent that K-feldspars should be more abundant than plagioclase since metamorphic lithics are present in higher percentages than igneous lithics. Furthermore K-feldspars are mineralogically more mature than plagioclase and thus more likely to be preserved. At Casino-3 in the base of Unit A there is minimal plagioclase (maximum 0.6%) but K-feldspar abundance does initially increase as depths become shallower until reaching a depth of approximately 2055m. After that depth there is a decline in feldspar abundance. There are similar increases in the percentage of feldspars at the base of Unit A in Casino-2.

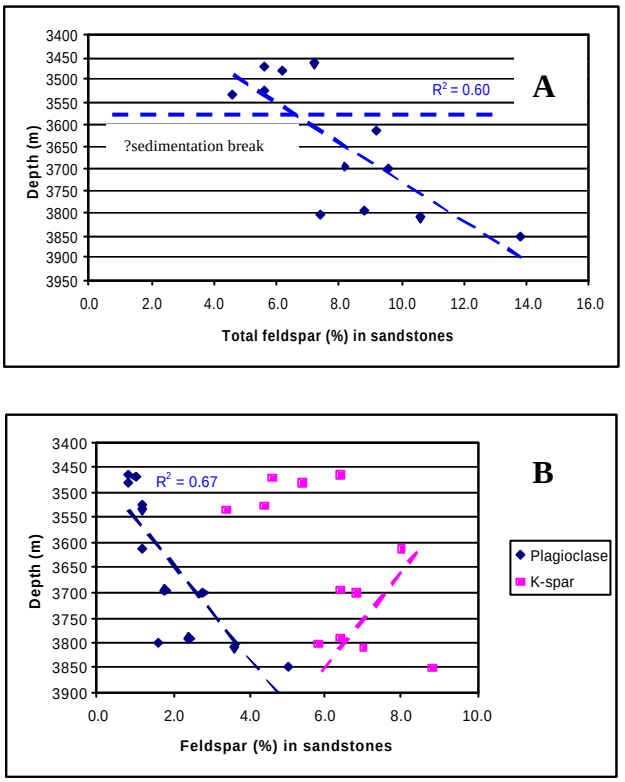

Figure 18. Relationships between depth and abundance (A)/type (B) of feldspars in sandstones at Callister-1

The trends noted in both feldspar and lithic abundance at the base of the Waarre Formation would appear to have regional significance and may serve to further subdivide the tectonostratigraphy.

Siltstones from Callister-1 (MSCTs 3, 11 & 17; depths 3858m, 3620m & 3482.6m) contain less lithics and feldspars than the sandstones. This characteristic might be a function of the hydraulic regime during deposition, rather than a difference in sediment provenance. Types of lithics and feldspars are very similar to those described from the sandstones therefore similar sources can be anticipated.

6.3 Depositional environments

A marine to marginal marine setting probably prevailed during deposition of sediments studied from Callister-1. Evidence from the petrology data and wireline logs might be consistent with either a lower delta plain influenced by distributary channels and/or a delta front.

The marine influence is apparent from the presence of minor to trace amounts of glaucony and rare pyrite framboids. Glaucony grains are commonly very fine to fine sand in size and vary significantly in colour from white through to dark green. Changes in colour are thought to reflect the maturity of the glaucony and thus the length of time it has been in contact with sea water during formation. Since glaucony forms at the sediment-water interface when sedimentation rates are low dominantly on continental shelves, it is possible that much of the glaucony is immature and has been reworked into these sandstones. In addition, there are instances where the glaucony appears to have been oxidised to goethite, probably during reworking. Exposure might have been more significant in the muddy siltstone of MSCT 3 (depth 3858m) because the burrow in this sample also contains a possible clay cutan. The latter would suggest at least initial soil formation processes operated after deposition.

Deposition probably occurred above mean fair-weather wave base as indicated by the presence of burrows with rare pellets. Possible vertical burrows and pellets are apparent in the muddy siltstone of MSCT 3 (depth 3858m) and a horizontal burrow may be present in the fine grained litharenite of MSCT 9 (depth 3700m). Pellets are also apparent in the muddy siltstone of MSCT 11 (depth 3620m). Higher percentages of organic matter in the siltstones would have encouraged the suspension and deposit feeders that could have made these dwelling burrows. It is possible that the burrows might characterise skolithos to cruziana ichnofacies.

Bedding and laminae (including ripple cross-lamination) are common in the sandstones and siltstones from Callister-1. It would appear that there were significant fluctuations in the hydraulic energy and currents of the depositional setting. When energy levels were low then organic matter and detrital clay associated with micas accumulated. The relative abundance of organic matter may suggest relatively close proximity to terrestrial environments.

Log signatures indicate both coarsening and fining upwards sequences with additional blocky channels eroded into underlying shales/mudstones. An example of the latter is evident at approximately 3590m which would be consistent with the proposed timing for a change in tectonic activity illustrated by trends in the feldspar and lithic contents of the sandstones. Distributary channels associated with deltas commonly display either coarsening and/or fining upward sequences.

Evidence for proximity to a river mouth (and hence delta) is apparent from the development of chlorite rims in sandstones from 3849.5m (MSCT 4) to 3695.5m (MSCT 10). Authigenic chlorite platelets oriented at right angles to the grain surfaces form distinctive rims up to 10 microns thick on intergranular pores. These rims are partially oxidised in the litharenites of MSCTs 7, 9 and 10 (depths 3791m, 3700m and 3695.5m) which were all taken from channel sands. Chlorite is thought to form where Fe transported from a terrestrial source via rivers is flocculated by the increase in salinity of sea water. This would suggest that the basal part of the sequence at Callister-1 was close to a river mouth but the shallower samples were more distal. Similar chlorite rims were noted at Pecten-1A and Martha-1 but these were probably not the same river mouth, although rivers may have had the same provenance.

6.4 Authigenic mineralogy & diagenetic alteration

Essentially the diagenetic sequence apparent from Callister-1 contains many of the elements already identified from the Casino Field, Pecten-1A and Martha-1. Early diagenetic phases of glaucony, pyrite, chlorite, oxidation and probably micritic Fe rich carbonate (?siderite) were related to the depositional environments. After burial the sediment was subject to mechanical compaction, dissolution, precipitation of kaolin, quartz, clear carbonate spar and traces of illite. There are two differences between the Casino Field and Callister-1. Feldspar overgrowths are absent from Callister-1, and there are no chlorite rims in the Casino Field. Feldspar overgrowths were thought to have formed due to the alteration/dissolution of volcanic lithics at Casino but this was not the case at Callister-1. Furthermore, there are variations in the relative proportions of authigenic minerals above and below the break in sedimentation noted between 3600 and 3550m in Callister-1.

Glaucony at Callister-1 generally appears to be relatively immature and in places oxidised. These characteristics indicate a relatively short time span which favoured glaucony precipitation and probable reworking by currents. Glaucony is a minor component of the sandstones and siltstones with percentages ranging from zero to 2.4% of the total rock composition (average 0.8%). Although there is slightly more glaucony above the sedimentation break this is not considered a significant difference (Table 3).

TABLE 3 Average percentage of authigenic minerals for sandstones & siltstones from Callister-1

Authigenic mineral	Average % below 3600-3550m N = 9	Average % above 3600-3550m N = 6
Glaucony	0.6	1.2
Chlorite - replace	4.1	1.3
- fill pores	4.2	0
Fe carbonate - replace	1.2	8.9
- fill pores	0	1.0
Clear carbonate - replace	2.3	4.8
- fill pores	1.0	1.0
Total carbonate	4.6	15.8
Quartz	0.4	1.0
Illite	0	0.2
Kaolin - replace	1.1	3.6
- fill pores	0.8	2.1
Oxide	0.5	0.1
Pyrite - replace	0	0.3
- fill pores	0	0.1

Replacement of detrital grains (lithics and feldspars) by chlorite and the precipitation of chlorite rims were more abundant below the sedimentation break. It is considered feasible that grain replacing chlorite formed at the same time as chlorite rims when pore waters were alkaline and there was minimal K^+ activity. Fe and Mg were probably derived from the alteration of mafic minerals within volcanic lithics for grain replacing chlorite. However, there are examples of chloritised quartzites which also suggest minor contributions of elements from metamorphic lithics. For chlorite rims the source of Fe is thought to have been associated with proximity of a river mouth and thus the concentration prior to the break in sedimentation. Chlorite rims formed prior to grain dissolution and are thus suspended around secondary pores. The fact that rims are absent at grain contacts suggests they precipitated after deposition of the sediment.

Fe rich carbonate (?siderite) is typically micritic but there is microspar and spar present and this phase of carbonate (0 to 19.8% of the total rock composition, average 4.1%) is thought to have precipitated prior to the clear spar. Typically Fe rich carbonate is concentrated in those fine grained samples where there is abundant detrital clay and/or organic matter which were probably the source of Fe. The dusty micrite has replaced grains and forms nodules up to coarse sand in size (eg MSCT, 15; depth 3535m). In addition, Fe rich carbonate is more abundant above the sedimentation break

(Table 3). The latter trend might suggest that the depositional environment was more strongly influenced by meteoric waters above the sedimentation break. Assuming the Fe rich carbonate is siderite then its presence reflects low sulphide activity that is found in fresh water, or where meteoric water is mixed with seawater. Glaucony in the same samples would suggest that there was mixing of fresh and sea water, perhaps due to a tidal influence. Micrite implies rapid rates of carbonate precipitation during this early phase of diagenesis and this lime mud can accumulate in a number of different environments from tidal flats to shallow lagoons. Fe rich spar formed more slowly and may have replaced the micrite during later diagenesis (aggrading neomorphism). Corrosion is evident in the Fe rich spar, especially above the sedimentation break (eg MSCTs 16 & 18; depths 3526.5m & 3481m). Dissolution indicates that pore waters temporarily became more acidic but there may have been more than one phase of corrosion. There is no evidence that siderite was corroded in the Casino Field.

Kaolin forms when pore waters are acidic and feldspars/micas become altered. Booklets range in diameter from 5 to 50+ microns at Callister-1 and size would have been determined by the nature of the grain replaced and rate of precipitation. Larger booklets developed where micas have been replaced and 5 micron size booklets probably represent rapidly altered feldspars. These small booklets are dominantly found within channel sequences (MSCTs 7, 9 & 10; depth 3791m, 3700m & 3695.5m). Higher percentages of pore filling and grain replacing kaolin occur above the sedimentation break (Table 3) especially in MSCTs 18, 20 & 21 (depths 3481m, 3471m & 3464m). Again this distribution could reflect stronger flushing by meteoric waters because the depositional environment had a terrestrial influence. Alternatively the upper part of the sequence was flushed by meteoric waters during later uplift and erosion. Kaolin formed after the chlorite rims below the sedimentation break and was squeezed into intergranular pores during mechanical compaction. The jagged contact between kaolin booklets and quartz overgrowths above the sedimentation break might suggest kaolin formed prior to quartz overgrowths. Trace amounts of illite associated with kaolin could reflect original zonation in the feldspars.

Rare prismatic quartz overgrowths formed after chlorite rims but before clear carbonate spar below the sedimentation break. Quartz overgrowths are more abundant in the same samples that have higher percentages of kaolin (MSCTs 18, 20 & 21) above the sedimentation break, which might indicate that the formation of these two authigenic minerals was related. When feldspars are altered to kaolin there is an excess of silica produced and this was possibly the source of silica for quartz overgrowths. It is clear that the proportion of quartz overgrowths does not increase with depth and therefore is not related to mechanical/chemical compaction.

Clear carbonate spar which appears to have formed after most other authigenic minerals (including Fe rich carbonate) has both replaced grains (feldspars) and filled intergranular pores. The poikilotopic nature of the clear spar suggests that it is burial cement and it appears to have formed after grain dissolution. Similar clear spar at Casino-3 was found to be composed of calcite. Clear spar has a relatively uniform distribution above and below the sedimentation break at Callister-1 and therefore was probably not influenced by depositional environments. It is possible that this carbonate phase was either related to CO_2 expelled in association with decarboxylation of organic matter prior to hydrocarbon migration, or CO_2 associated with Pleistocene to Recent igneous activity (Watson *et al*, 2004). Isotopic analyses would aid in the differentiation of carbon sources. High levels of pCO_2 can cause carbonate dissolution. Therefore it is possible that this late CO_2 pulse initially dissolved the earlier Fe rich carbonate and then as CO_2 levels were buffered the clear spar precipitated. This hypothesis would be consistent with an igneous source of CO_2 since there are known Pleistocene to Recent volcanoes just off the coast of Portland (Watson *et al*, 2004) near Callister-1, but there are no volcanoes near the Casino Field.

Trace amounts of framboidal pyrite were noted in four samples from Callister-1 and only in MSCT 21 (depth 3464m) is blocky pyrite evident. Framboidal pyrite is thought to be very early diagenetic and related to the marine/marginal marine depositional environments. Pyrite forms when bacteria reduce sulphate in sea water and sulphide is combined with Fe from detrital clays and organic matter. In contrast, blocky pyrite is thought to be late diagenetic and in MSCT 21 it appears to postdate the clear carbonate spar. In this instance it is possible that sulphate reducing bacteria have been recently

introduced to the system and these are reacting with remnants of reservoir bitumen or other organic matter.

The possible paragenetic sequence as recognised at Callister-1 is summarised in Table 4 below. Not all diagenetic phases and authigenic minerals are present in each sample studied. Depositional environments are thought to have strongly influenced many of the early authigenic minerals.

TABLE 4 Paragenetic sequence for sandstones and siltstones from Callister-1.

Event	Diagenetic Stage Early	Middle	Late
glaucony	---		
pyrite	---		----
chlorite	----		
Fe rich carbonate	----		
oxidation/dissolution	----	----	
kaolin	----		
quartz	----		
uplift in metamorphic source ceased	---		
mechanical compaction	----------		
CO2 charge		---------	
clear carbonate spar		-----	

6.5 Reservoir quality

Routine core analyses indicate porosity ranges from 6.7 to 17.2% and permeability from 0.07 to 2.66 (mD) in the sandstones and siltstones from Callister-1. These results are not directly comparable with the petrology data because only porosity can be determined from thin section. Furthermore, porosity is measured in two dimensions in thin section but three dimensions in core analysis, therefore it is common for core analysis values to be higher. The most significant contribution from the thin section data is the type of pores present and their relative proportions (Fig. 19). At Callister-1 it is clear that porosity is dominated by secondary dissolution pores (average 4.8%, range 0 to 8.8%). These pores include grain size dissolution pores, honeycomb pores within corroded feldspars and intragranular pores within lithics. Secondary pores are very poorly (if at all) interconnected and thus permeability values are low.

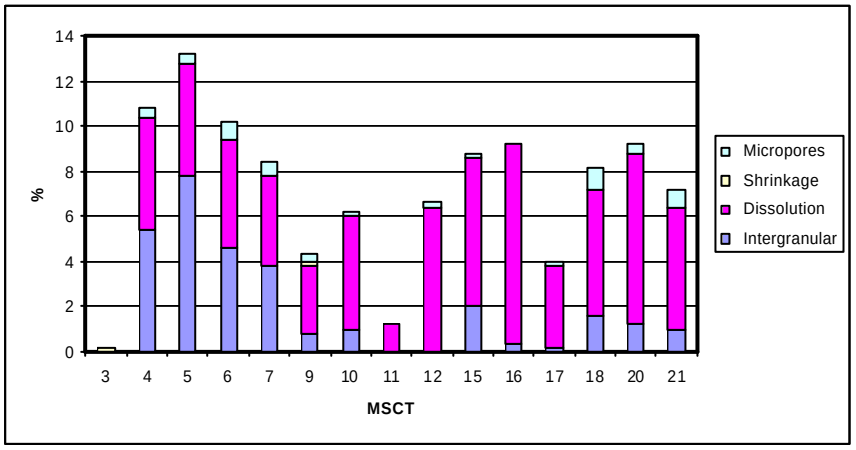

Figure 19. Pore types in the sandstones and siltstones of Callister-1 as identified from thin section

Dissolution pores are more abundant (average 6.3%) above the sedimentation break (between MSCTs 12 and 15), than below (average 3.8%). Furthermore, there are a significant number of secondary pores (6.4%) in the litharenite (MSCT 12, depth 3614m) immediately below the break.

These observations might suggest there was flushing and dissolution of underlying sediments when there were breaks in sedimentation. For MSCT 12 this might have been associated with the end of uplift in the metamorphic terrane.

Minor permeability has been retained where there are higher percentages of primary intergranular pores (Fig. 19) in MSCTs 4, 5, 6 and 7 (depths 3849.5m, 3809.5m, 3802m and 3791m). These intergranular pores are preserved where there are chlorite rims representing 6 to 9.6% of the total rock composition (Fig. 20). Those samples with less pore riming chlorite (MSCTs 9 & 10; depths 3700m & 3695.5m) have significantly less intergranular porosity. However, intergranular porosity represents up to 2% when chlorite rims are completely absent (Fig. 20). These intergranular pores in some instances (eg MSCT 15, depth 3535m) are not primary, but have redeveloped after dissolution of pore filling carbonate cements. Intergranular pores are also better preserved (1.0-1.6%) where there are minor quartz overgrowths in MSCTs 18, 20 & 21 (depths 3481m, 3471m & 3464m). Therefore both chlorite rims at depth and quartz overgrowths in the shallower sediments were responsible for preserving primary intergranular pores. However, in both instances there was not enough intergranular porosity to retain good permeability.

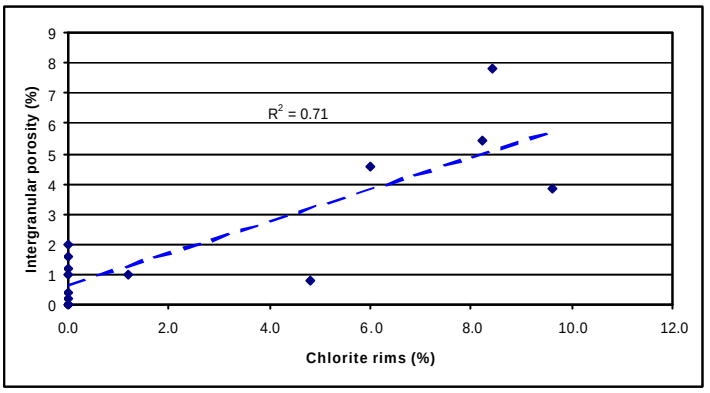

Figure 20. Correlation between chlorite rims and intergranular pores in sediments from Callister-1.

Primary intergranular pores at Callister-1 have been occluded by a combination of compaction (plastic deformation of ductile grains, grain fracturing, pressure solution and grain rotation/slippage) and pore filling cements (carbonate, chlorite, kaolin and quartz). Grain packing described from thin section is moderately close to close throughout the sequence and there is no significant increase in compaction with depth (Fig. 21a). This might suggest that compaction was the dominant influence on loss of intergranular porosity throughout the sequence. Compaction loss was calculated using the method of Lundegard (1992). When compaction loss is compared to total pore filling cements in the sandstones from Callister-1 (Fig. 21b) it is evident that there is no significant trend apparent. Compaction loss was typically not influenced by the amount of pore filling cement and therefore was probably the primary control of reservoir quality.

Micropores associated with pore filling kaolin and chlorite (average 0.4% total rock composition) did not significantly increase total porosity. Furthermore these clays would have reduced permeability by blocking pore throats when compacted.

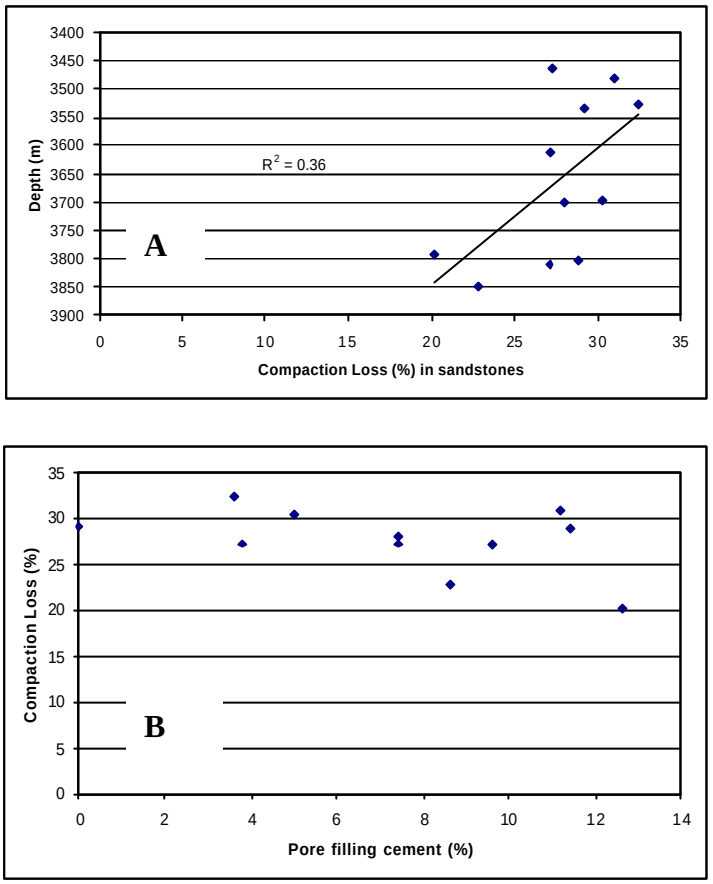

Figure 21. Influence of compaction on the loss of intergranular porosity in sandstones from Callister-1.

7. CONCLUSIONS

1. Sandstones from Callister-1 are very fine to medium grained, poor to well sorted litharenites and feldspathic litharenites. Muddy siltstones are also apparent and interbedded with the sandstones.

2. Sediment was derived dominantly from a metamorphic terrane with lesser igneous influence. Distinctive trends in feldspar and lithic contents at the base of the sequence suggest a change in sedimentation at approximately 3600 to 3550m, possibly associated with tectonic activity in the metamorphic area. Very similar trends and lithic types were apparent in the Casino Field and may reflect regional trends in the tectonostratigraphy.

3. A marine to marginal marine depositional environment of either a lower delta plain influenced by distributary channels and/or a delta front is envisaged for sediments from Callister-1. Initial deposition probably occurred close to a river mouth and shallower sediments had a more terrestrial influence.

4. Trends in early diagenetic alteration (glaucony, pyrite, chlorite, Fe rich carbonate and oxidation) were related to the depositional environments and other relationships could have been influenced by the break in sedimentation. After burial the sediment was subject to compaction, dissolution and precipitation of kaolin, quartz and clear carbonate spar. Dissolution of feldspars might be related to flushing by meteoric waters after uplift and corrosion of Fe rich carbonate could have occurred in association with a pulse of CO_2 attributed to localised Pleistocene to Recent volcanism.

5. Poor reservoir quality at Callister-1 is the result of primary intergranular pores being occluded by compaction. Porosity is dominated by secondary dissolution pores (grain size, honeycomb and intragranular) which are poorly interconnected. Remnants of intergranular pores are preserved where there are chlorite rims at depth, or quartz overgrowths in shallower samples and these samples have minor permeability.

8. GLOSSARY OF TERMS

Framboid
A cluster of pyrite crystals with a spheroidal outline.

Glaucony
A term used to describe green minerals without any genetic connotations. If the green minerals can be identified, a specific mineral name is given.

Glauconite
An Fe-rich dioctahedral illite. The term is also used to refer to a family of Fe-rich dioctahedral clays with varying ratios of expanded (smectite) and non-expanded layers.

Granophyric Texture
A variety of micrographic intergrowth of quartz and alkali feldspar that is either crudely radiate or is less regular than micrographic texture.

Honeycomb Porosity
Secondary porosity produced by the corrosion (etching) of detrital grains.

Micrographic Intergrowth
A regular intergrowth of two minerals.

Microporosity
Porosity directly associated with clay minerals.

Neomorphism
All transformations between a mineral and the same mineral, or another of the same general composition.

Poikilotopic
A sedimentary textural term denoting a single crystal of carbonate enclosing more than one framework grain.

Spherulitic
The presence of more or less globular masses of generally acicular crystals, having a radial arrangement. spherulites form as a result of devitrification of volcanic glass.

Trachytic
A textural term applied to the groundmasses of volcanic rocks in which there is a subparallel arrangement of microcrystalline, lath shaped feldspars. The term is not restricted in use to rocks of trachyte composition.

9. REFERENCES

ADAMS, A.E., W.S. MACKENZIE & C. GUILFORD (1984) *Atlas of sedimentary rocks under the microscope*. Longman Scientific & Technical, 104p.

FOLK, R.L. (1974) *Petrology of sedimentary rocks.* Hemphill, 182p.

HARRELL, J. (1984) A visual comparator for degree of sorting in thin and plane sections. *Journal of Sedimentary Petrology*. 54, pp. 646-650.

LUNDEGARD, P.D. (1992) Sandstone porosity loss – a "big picture" view of the importance of compaction. *Journal of Sedimentary Petrology*, 62, pp. 250-260.

PETTIJOHN, F.J., P.E. POTTER & R. SIEVER (1987) *Sand and sandstone*. Springer-Verlag, New York, 553p.

PHILLIPS, S.E. (2003) Petrology report Casino-1 & Casino-2, Otway Basin (VIC/P 44). Confidential report (number 087) by PGPC for Santos Ltd, 81p.

PHILLIPS, S.E. (2004a) Petrology report Casino-3, Otway Basin (VIC/P 44). Confidential report (number 099) by PGPC for Santos Ltd, 117p.

PHILLIPS, S.E. (2004b) Petrology report Pecten-1A, Otway Basin. Confidential report (number 0104) by PGPC for Santos Ltd, 20p.

PHILLIPS, S.E. (2005) Petrology report Martha-1, Otway Basin. Confidential report (number 0110) by PGPC for Santos Ltd, 37p.

STANTON, P.T. & M.D. WILSON (1994) Measurement of independent variables - composition. In M.D. WILSON (Ed) Reservoir quality assessment and prediction in clastic rocks. *SEPM Short Course* 30, 432p.

TERRY R.D. & G.V. CHILINGAR (1955) Summary of "Concerning some additional aids in studying sedimentary formations" by M.S. Shrestor. *Journal of Sedimentary Petrology*, 25, pp. 229-234.

TUCKER, M.E. (2001) *Sedimentary petrology, an introduction to the origin of sedimentary rocks.* (3rd Ed) Blackwell Scientific, 262p.

WATSON, M.N., C.J. BOREHAM & P.R. TINGATE (2004) Carbon dioxide and carbonate cements in the Otway Basin: implications for geological storage of carbon dioxide. *The APPEA Journal*, 44, 1, pp. 703-720.